POTENTIAL FOR SLUMPS, SEDIMENT VOLCANOES, AND EXCESS TURBIDITY IN THE NEMADJI RIVER BASIN

A THESIS
SUBMITTED TO THE FACULTY OF THE GRADUATE SCHOOL
OF THE UNIVERSITY OF MINNESOTA
BY

Irvin Gerald Mossberger

IN PARTIAL FULFILLMENT OF THE REQUIREMENTS
FOR THE DEGREE OF
MASTER OF SCIENCE

Dr. Howard Mooers

June 2010

Acknowledgements

I would like to thank the following: Mr. Johnson, my 3rd grade science teacher, who, after viewing how I colored alternating shale and limestone units for a class assignment said, “You’ll be a geologist yet, son.” I’d also like to thank Mr. Rick Lange, whose slides of his trip to the Brooks Range in Alaska in his Geology elective at Superior Senior High School inspired a love in me for Geology, enough to choose it as my career. Thanks to Dr. Lung S. Chan formerly at the University of Wisconsin-Eau Claire, who made me promise not to give up on Geology. Next, my advisor Howard Mooers who, despite my slow pace, was always supportive and helped me with anything I asked of him. Much gratitude goes to my committee, Nigel Wattrus and Steve Sternberg, for their advice, encouragement, and time. Thank you to the University of Minnesota-Duluth Department of Geological Sciences faculty and staff for funding and assistance. Thanks go to Joan Weyandt and Kirstin Swenson of the CCSWCD, who provided much information and support. I am grateful to the managers and employees of Service Engineering Group and Barr Engineering for their interest in my topic and progress, for giving me a job to support myself, and for time off to work on this project. Much appreciation goes to my fellow graduate students and friends, too numerous to list, for lending technical and moral support, including Andrea Grygo and David Noto. To Carrie Mohn, who assured me it was alright to work on this in my own time and fashion. I’d like to thank Randy’s Café in West End and Beaner’s Café in West Duluth for providing food, caffeine, and comfortable environments in which to write.

Foremostly, I’d like to thank Maria Vuldjeva. Her meeting with Howard in Birmingham during UMD’s Study in England program was the impetus for me to apply at UMD, which was my goal ever since graduating from UWEC. Despite difficulties, she supported me for so many years and made my life much richer than I could’ve ever possibly imagined. Though our lives have gone in different directions, I dedicate this thesis to her.

Abstract

Beginning in the early 1990's, a portion of Deer Creek, a tributary of the Nemadji River in the Lake Superior basin, experienced the formation of sediment volcanoes in its creek bed, along with related slumping, enhanced erosion rates, and turbidity in excess of state total maximum daily load (TMDL) limits. Slumping near the stream has increased erosion rates and may eventually threaten the stability of nearby structures. The resulting excess turbidity negatively impacts aquatic wildlife, and increases sedimentation rates and dredging costs in downstream navigable waters.

Slumping and formation of sediment volcanoes at Deer Creek were likely caused when dynamite was used to destroy a nearby beaver dam on the creek. Some combination of rapid pond drainage and/or disturbance from the explosives may have led to fracturing of a glacio-lacustrine clay confining layer over a locally extensive aquifer. A sediment volcano and associated slumping are also present along nearby Mud Creek. The sediment volcano areas at Deer and Mud Creeks both occur at the toe of 10-meter high slumps. The failure planes of these slumps may facilitate formation of sediment volcanoes by providing pathways for groundwater to reach the surface. Predicting slump locations should then also help predict the location of potential sediment volcanoes.

The stratigraphic and hydrologic conditions in Deer and Mud Creeks are similar to those throughout nearby areas in the Nemadji River basin. This project examines the relationship between the slumps and sediment volcanoes, and develops a predictive model of the potential for slope failure in the lacustrine clay portions of the basin. A 3-D model of stratigraphy and hydraulic potential from more than 300 wells is used, along with slope stability analysis with the stress-slope and Mohr-Coulomb equations in a GIS.

Results of the modeling found higher susceptibility for slumping in areas of high slope and high potentiometric surface. The model correlated well at a 92% rate with a data set of 322 inventoried slumps, and included both volcano areas, without overpredicting high-risk slump areas. Another model, SINMAP 2.0, was run to test the veracity of the original model's results. Both models were in good agreement with each other. This project provides a reasonable approximation of slope stability and can be used to assist in land use planning to help reduce erosion and its consequences.

Table of Contents

List of Tables

List of Figures

INTRODUCTION

The Nemadji River, known as the “Left Hand” River in Ojibwe language, drains the former bed of glacial Lake Duluth (Farrand, 1969), then enters the Duluth-Superior Harbor on its way to Lake Superior (Figures 1 and 2). The river is on the left hand as one approaches it from historical fur trading routes on Lake Superior, with the St. Louis River, which also flows into the harbor, on the right (Upham, 2001). Most of the Nemadji’s watershed is located in Carlton County, Minnesota, and the mouth is in Douglas County, Wisconsin. The Nemadji and its tributaries are deeply incised into red clay of the former lake bed, often forming steep stream banks with exposed clay (Figure 3). The exposed clay is susceptible to slumping and accelerated erosion. Two known sediment volcano areas (Figures 4 and 5) are located at the toes of slumps along the Deer and Mud Creek tributaries of the Nemadji River. The volcanoes contribute a significant amount of sediment to the overall stream load (Mooers and Wattrus, 2005).

Although a multitude of erosion-related studies have been conducted in the Nemadji River basin, emphasizing such factors as land use, stream metrics, etc. (e.g., Wold, 1994; Reidel, 2005; Magner and Brooks, 2007), none have focused on basin-wide quantitative hillslope stability and erosion susceptibility, and none have generated models in GIS map format for ease of use for land use planners.

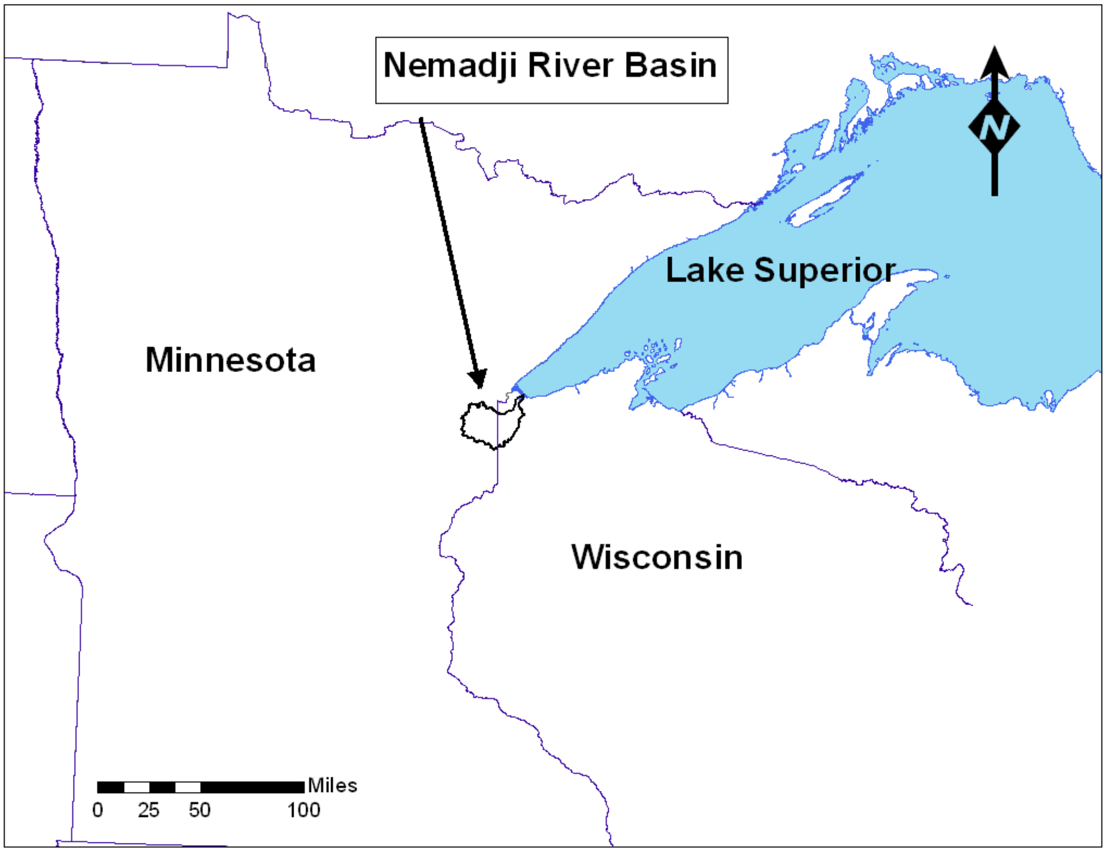

Figure 1. Site Location Map.

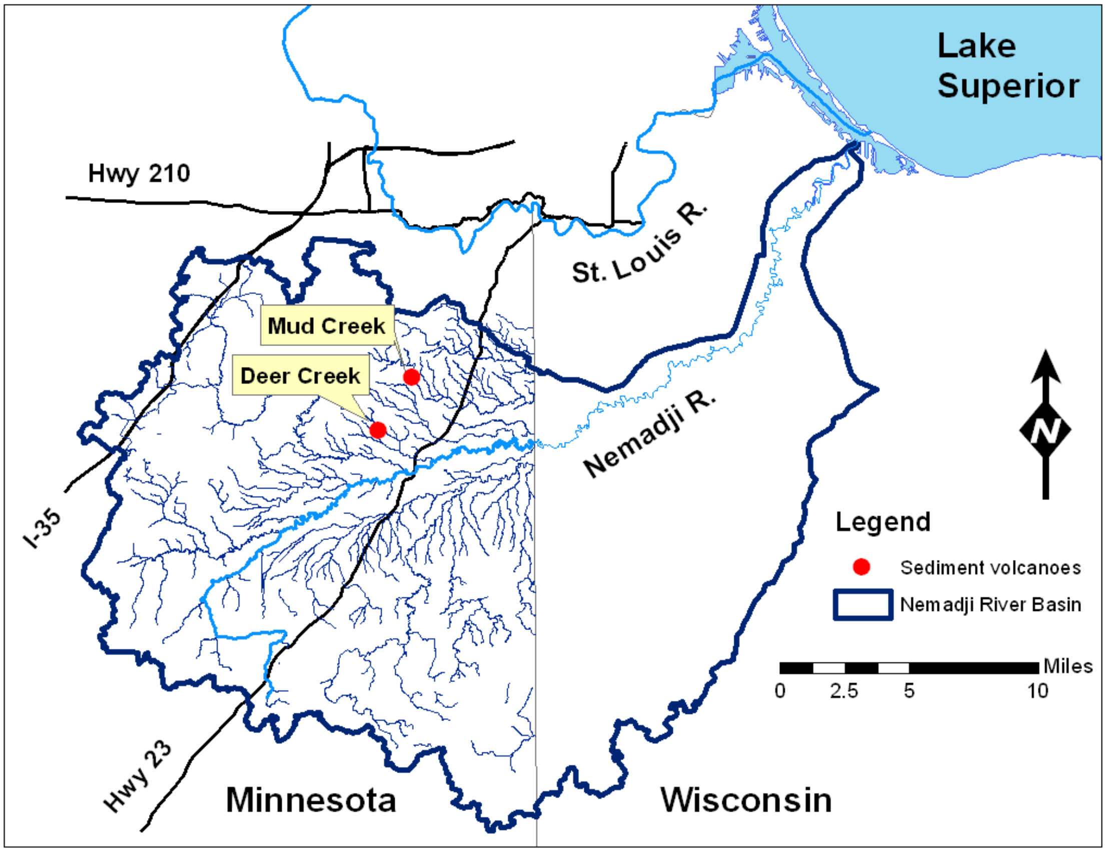

Figure 2. Nemadji River Basin Detail.

Figure 3. Typical slumping on the Nemadji River.

Figure 4. Sediment volcano at Deer Creek.

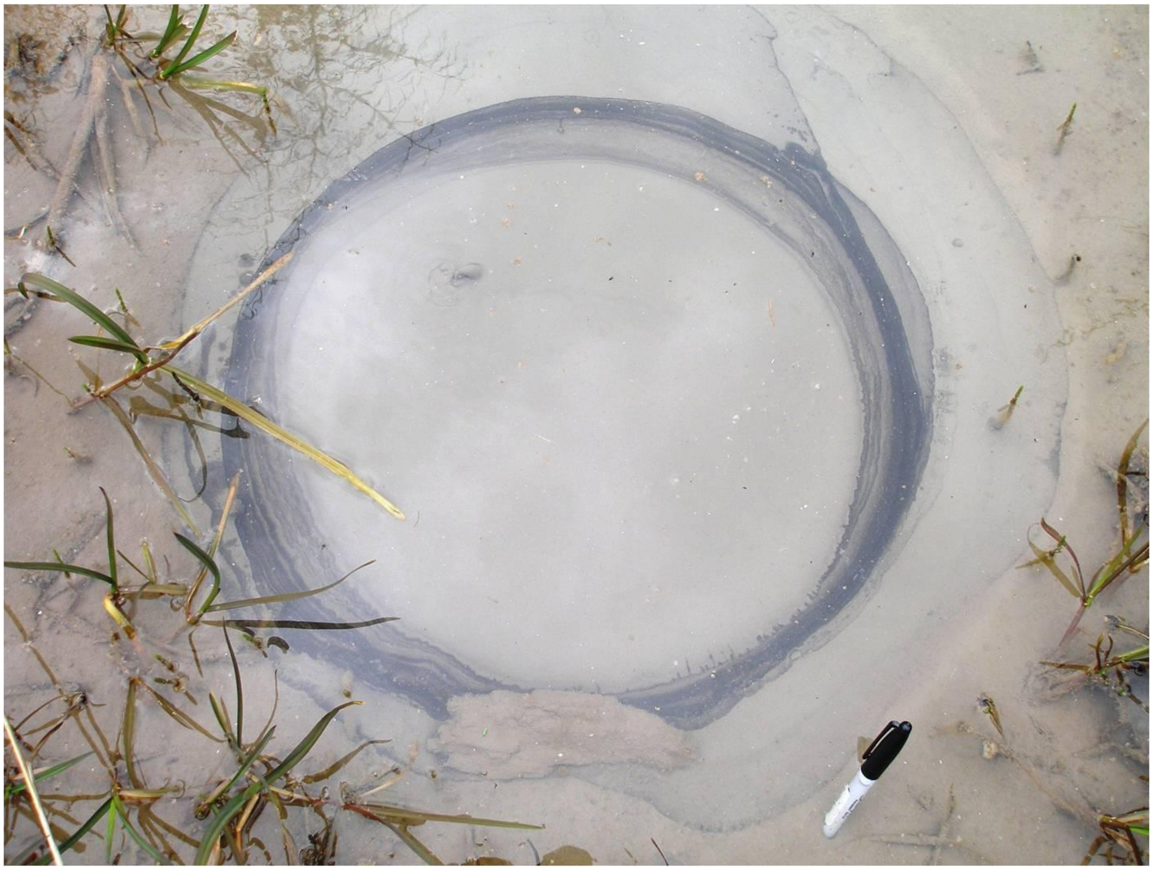

Figure 5. Sediment volcano at Mud Creek.

Project Objectives/Hypothesis

This project builds upon a study of Deer Creek by Mooers and Wattrus (2005). Their investigation included analysis of slope failure potential along a cross-section near Deer Creek using the Mohr-Coulomb failure criterion to determine areas susceptible to slumping. Since most of the Nemadji River basin is located in the former bed of glacial Lake Duluth, most of the streams in the Nemadji River basin flow through the same geologic and hydrologic regimes as Deer Creek.

This study examines the relationship between the volcanoes and slumps, and attempts to provide a quantitative predictive model for slumping in the red clay portion of the Nemadji River basin using the Mohr-Coulomb and stress slope equations in a

Geographic Information System (GIS). Such a model can be used by stakeholders and other interested parties such as citizens, government agencies, and developers for land use management to identify and limit activities that cause slumping, erosion, and excessive turbidity in the basin.

Problem

Slumping of stream banks, such as those in the Nemadji River, increases erosion and downstream sedimentation by supplying freshly exposed sediment to the stream (Easterbrook, 1999). Slumping and erosion can threaten the stability of nearby structures (Figure 6). If a slump intersects a confined aquifer, water under high hydraulic head in the confined aquifer can then seep to the surface, contribute baseflow, and increase the sediment load to the streams.

Sedimentation from the Nemadji River deposits about half of the sediment yielded to the Duluth-Superior harbor (NRCS, 1996), and causes various economic and environmental problems. For example, a large plume of suspended sediment from the river is often visible in Lake Superior after rainstorms (Figure 7).

One economic impact of excessive turbidity in the Nemadji River is the cost of dredging. Dredging is necessary to maintain adequate draft for ships that use the 17 miles of harbor shipping channels. Insufficient draft requires ships to reduce their cargo load, leading to increased transportation costs. The United States Army Corps of Engineers (USACE) has estimated that approximately 33,000 tons of sediment each year is dredged from the Duluth-Superior harbor (NRCS, 1998). The Nemadji's contribution to the dredged sediment is approximately 19,000 tons, or 1,000 dump-truck loads, of sediment to the harbor annually, resulting in a burden to taxpayers for dredging and disposal of the Nemadji's sedimentation. Federal funding for Upper Great Lakes dredging was cut nearly in half in 2009, adding to the dredging backlog that has developed in the harbor (Duluth News-Tribune, 2008).

Disposal of dredge spoils is another economic impact of the Nemadji's high sediment load. The USACE's current dredge disposal facility for the harbor, Erie Pier, is expected to run out of capacity in 2017 due to the accumulation of excess fine-grained material (DSMIC, 2007).

Figure 6. Repaired slump on Highway 23 at the South Fork of the Nemadji River.

Figure 7. Plume of sediment from Nemadji River in Lake Superior (USGS). June, 1997.

In addition to economic impacts, sediments can cause environmental problems. Suspended sediments are considered non-point pollution when they occur in high enough concentrations in designated surface waters. Industrial pollutants such as mercury, dioxins, and PCBs can attach to sediment particles, trapping toxins or oxygen-demanding materials in the harbor (Bridges, 2008; WDNR, 2008). Dredging agitates and re-suspends settled pollutants, elevating toxin levels in the water and biota (MPCA, 1992). The Minnesota portion of the Nemadji watershed represents approximately 40% of Lake Superior's migratory trout and salmon spawning habitat in Minnesota (Carlton County Water Plan Advisory Committee, 2000). Fine-grained sediments from the Nemadji can clog fish gills and degrade the quality of lake trout and herring spawning bed habitat by suffocating eggs.

In June, 2009 the USACE complied with a Minnesota Department of Natural Resources (MnDNR) request to cease depositing dredge spoils from the Duluth-Superior harbor onto the nearby beach on Lake Superior due to concerns for fish habitat. The high silt and clay content (30-40%) of the spoils became suspended in Lake Superior creating a highly visible turbidity plume spreading across several miles (Duluth News-Tribune, 2009).

The harbor became one of the 43 Areas of Concern (AOC) under the Great Lakes Water Quality Agreement (WQA) in 1972. In 1987, Remedial Action Plans (RAPs) were developed to improve the health of the Nemadji and St. Louis Rivers. The harbor was designated as impaired for five uses, including fish consumption advisories, degradation of benthos, restrictions on dredging, degradation of aesthetics, and loss of fish and wildlife habitat (NRCS, 1998).

Total Maximum Daily Load (TMDL)

In December 2003 the Minnesota Pollution Control Agency (MPCA) added the Nemadji River and Deer Creek to the federal Clean Water Act 303d list of impaired waters for turbidity (MPCA, 2004). Turbidity is a numeric criterion used to assess the water quality condition of streams; it is a measure of the degree to which water loses its transparency due to the presence of suspended particulates. The federal Clean Water Act (CWA) requires states to adopt water-quality standards to protect waters from pollution (MPCA, 2008). These standards are called a Total Maximum Daily Load (TMDL). A TMDL defines maximum permissible amounts of pollutants that still allow the water body to meet designated uses, such as drinking water, fishing and swimming. The standards apply to a wide range of pollutants, including bacteria, nutrients, turbidity and mercury. A water body is considered to be “impaired” if it fails to meet one or more water quality standards. Section 303(d) of the Clean Water Act requires states to: 1) assess all waters of the state to determine if they meet water-quality standards, 2) list waters that do not meet standards (also known as the 303d List), 3) conduct TMDL studies in order to set pollutant reduction goals, and 4) implement restoration measures to meet TMDLs.

Passing of the Clean Water Amendment in Minnesota in 2008 provided nearly 20 million dollars in funding for TMDL development for Fiscal Year 2010-2011. In January 2008 the Carlton Soil and Water Conservation District (SWCD) entered into a contract with MPCA to conduct Phase I of a TMDL study for the Nemadji River and Deer Creek impaired waters listings. In spring, 2008 work began on the Deer Creek portion of the study.

In 2008, the Carlton County Soil Water Conservation District (CCSWCD) found that turbidity readings upstream of the Deer Creek sediment volcanoes ranged from 7 to 105 nephelometric turbidity units (NTUs), and readings downstream ranged from 31 to 466 NTUs, a four-fold increase. Water clarity measured with a Secchi disk dropped from 54 cm (22 in) to 13 cm (5 in) downstream from where Deer Creek enters the North Fork of the Nemadji River, again a four-fold difference. Monitoring conducted by Nemadji River Basin Project (NRBP) staff in 2004 showed that total suspended solids in Nemadji streams typically have less than 40 milligrams per liter (mg/L) of water, whereas Deer Creek was above 600 mg/L, a fifteen-fold difference (CCSWCD, 2005).

In 2009 a sampling/monitoring work plan was completed. The Draft TMDL is targeted to be completed by 2012.

Sediment Volcanoes

There are several different structures created in nature by geo-excreted fluids that deposit material around the discharge point in formations that resemble volcanoes. The structures are generally associated with short-term increases in hydraulic pressure below a confining layer (Kappel, 1996). The processes forming the structures include earthquake liquefaction and escape of groundwater (Bolt, 1993), volcanic activity such as geothermal geyser venting (e.g., Yellowstone Park), methane offgassing on continents and in oceans, and freeze-thaw in permafrost. Recent images taken by NASA's Mars Odyssey spacecraft suggest the presence of methane-generating mud volcanoes on Mars (Allen, et al., 2009). Those found in the Nemadji River basin are formed from focused discharge of groundwater under artesian pressure.

There are several different names for these geologic structures. The names vary regionally and with the processes that create them. A literature review indicates there is no standardization in the terminology. The terms encountered included mud volcano (Milikov, 2000), mud pot (Raymahashay, 1968), mud boil (Kappel, 1996), sand volcano (Gill and Keunen, 1957), sand blow (Saucier, 1989), sand boil (Li, et al., 1996), sand springs (Guhman and Pederson, 1992), and hydrodynamic blowouts (Bluemle, 1993). For standardization purposes, I propose using the term "sediment volcano" herein for the structures at Deer and Mud Creek.

Sediment volcanoes have been documented in association with slumps in places such as the Caspian Sea (Corthay and Aliyev, 2000), the Namurian basin of Ireland (Strachan, 2002), and Onondaga County, New York; (Kappel, et al., 1996). Land subsidence can occur as groundwater escaping the aquifer causes the aquifer to depressurize and subside (Kappel, et al., 1996). This process can threaten the stability of nearby structures as evidenced by a bridge collapse in Onondaga County in 1991 (Kappel, et al., 1996).

Since the early 1990's, an area along Deer Creek has experienced extensive bank failure by slumping, and the formation of sediment volcanoes (Figure 4). Focused groundwater discharge under artesian pressure is occurring at the surface expression of slump faults around the perimeter of a former beaver pond. Typical displacements along the fault scarps at Deer Creek were found to be from 1 to as much as 3 meters (Mooers and Wattrus, 2005). Coarse sediment transported by the groundwater is deposited near the discharge point, forming volcano-shaped structures, while finer sediment remains in suspension, causing excess turbidity in the creek. Escaping groundwater dewaters the sandy confined aquifer, causing subsidence and leading to more slumping in a positive feedback process. On the order of ten sediment volcanoes have been observed at the Deer Creek pond at various times in the years 2006 to 2008.

A sediment volcano is also located at the toe of a slump approximately two miles away from the Deer Creek volcanoes in nearby Mud Creek. Mud Creek is also a tributary of the Nemadji River, and runs roughly parallel to Deer Creek (Figure 8). Both of the sediment volcano areas occur near the northern boundary of the clay extent in the basin (see Glacial Geology, following) and both areas are in the elevation range of 900 to 950 feet above mean sea level (asl).

The discharge points of the Deer Creek sediment volcanoes range in size from a few millimeters to an estimated 10 meters in diameter. The Mud Creek sediment volcano is approximately 1/3 meter in diameter. The discharge points can be transitory, and can shift locations as they erode their surroundings and exploit various other fractures. Discharge varies seasonally and by the size of the discharge point. The Deer Creek sediment volcanoes were collectively estimated to discharge approximately 100 gallons per minute to the creek (Mooers and Wattrus, 2005).

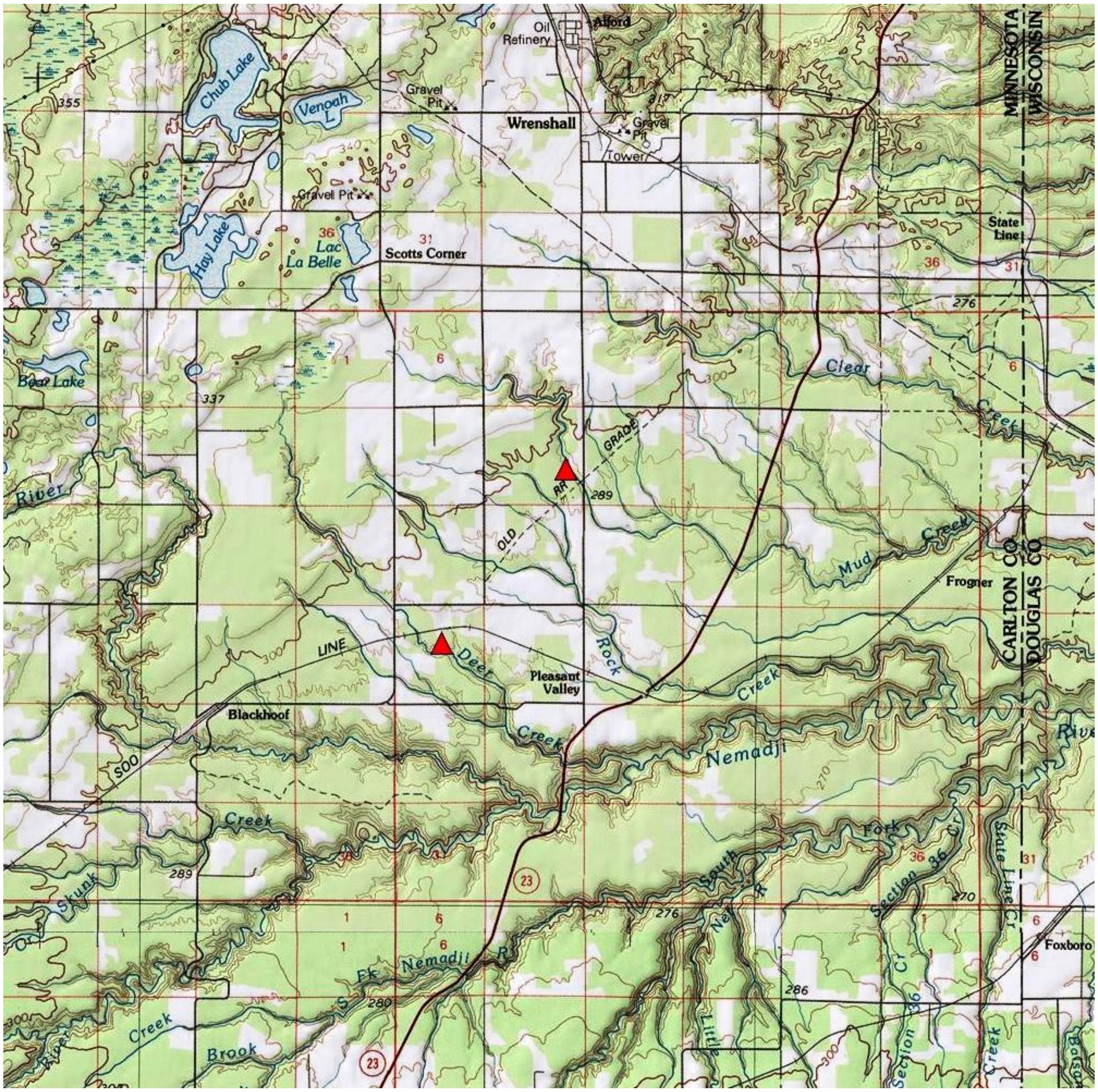

Figure 8. Topographic map with red marks showing the approximate locations of the Deer and Mud Creek sediment volcanoes. Each grid square is approximately one mile square.

Previous and Concurrent Work

Numerous investigations have addressed mass wasting, erosion, or high suspended sediment loads in the Nemadji River and its tributaries. In December 2008, a document issued by the CCSWCD (Swenson, 2008) listed and ranked 43 past reports containing information related to the high turbidity levels in the Nemadji River basin. This section discusses some of the pertinent reports along with other work conducted in the basin.

The Wisconsin Red Clay Interagency Committee worked from 1958-1967 on structural projects including culverts and water retention devices (dams) to reduce peak flows and trap sediment in basins (sediment dams, tile drains in road ditches, rock-filled cribs). Today, many of these basins are near or exceeding sediment capacity (NRBP 2004). Some of the dams have been poorly maintained and steel pipes in the culverts have exceeded their lifespan and are rusting away.

In the 1970's a multi-agency program called the Red Clay Project was initiated across the south shore of Lake Superior to study shoreline and stream erosion of red clay banks. In the Nemadji watershed, the project focused on Skunk Creek, a tributary to the Nemadji River. A total of sixteen (16) reports on such topics as stream flow and water quality monitoring, soil surveys, roadside erosion, erosion control, clay flocculation, slope stability, and vegetation effects on water content and soil stability were issued as part of the Red Clay Project (Andrews, 1980).

Banks and Brooks (1992) summarized past research of the area, and collected new data to reassess the Red Clay Project findings. The new data documented a dramatic increase in turbidity in Deer Creek, from 52 to 1283 NTUs. They also developed sediment rating curves - empirical relations between the total (fluid) discharge and the sediment discharge - and promoted the value of reducing upland runoff in smaller events through vegetative management. Dams were somewhat effective in reducing sediment loads, but inhibited trout migrating upstream.

Wold (1994) used simple linear regression models of slump frequency in relation to land cover, watershed area, channel gradient, time of concentration, slope, and sediment concentration to determine that the number of slumps in nine (9) Nemadji River subwatersheds increased as the percentage of non-forested area in the subwatersheds increased. Site-specific activities such as road construction and logging appeared to have the greatest effect impact in areas with steeper slopes in red clay soils. Significantly, slump occurrence was found 98% of the time to be located below 1000 feet in elevation, the approximate upper boundary of the red clay extent. Wold mapped 137 slumps in the nine sub-watersheds. Wold also found a strong correlation (96%) between turbidity and TSS in his water samples from the Nemadji.

In 1994 the NRCS and other agencies began work on the Nemadji River Basin Project (NRBP) with the mission of recommending "remedial actions and treatments to implement restoration to beneficial uses of the Nemadji River Basin." A report was issued summarizing the Phase I findings (NCRS, 1998). A sediment budget for the project identified that 89% of the 132,000 tons of fines eroded from the Nemadji River basin came from erosion along streams, and 11% from roadside, sheet, and rill erosion. Of the erosion along streams, 92% was attributed to the red clay portion of the Nemadji River basin.

The Phase I study concluded that hydrologic changes caused by human activities such as deforestation from logging and agriculture, and clearing streams of debris for log transport resulted in increased volumes and rates of runoff and streamflow that increased erosion and slumping. The study estimated a 10-fold increase in sedimentation rate following European settlement, but a decrease since approximately 1950 from reduction in agriculture and reforestation. Recommendations from the report included stabilizing runoff volumes and peak discharges through land use management including forestry, agriculture, wetlands, erosion control, and beaver management.

In 1999 a Phase II Workplan draft for the NRBP was issued that promoted goals of habitat and water quality inventory, restoration, and monitoring. The NRBP ended in 2006.

Baird & Associates (2000) assessed the effects of land use change on the hydrodynamics and sediment transport in the Nemadji River. The project linked hydrologic, hydrodynamic, and sediment transport models. The sediment transport models were completed for the Deer and Skunk Creek tributaries using GIS and the Danish Hydraulic Institute MIKE 11 System. The model required specialized training and was presented at a training session. Its usefulness was questioned by workshop attendees at the time it was presented.

In 2001 and 2002, the Minnesota Department of Natural Resources (MnDNR) conducted a helicopter survey of slumps along the North and South Forks of the Nemadji River and three of its tributaries. Photographs of 185 slumps were linked to a location map of the slumps. The data is unpublished but resides at the MnDNR fisheries office in Two Harbors, Minnesota.

Riedel (2000) studied the effects of riparian land use conversion on the morphology and stability of clay channel streams. He used stream cross-sections, grain size analysis, and analysis of root contribution to streambank stability using a modified form of the Mohr-Coulomb equation, the infinite slope method, an approach that ignores porewater pressure. Reidel used values for cohesion of 11-13 kPa which are 2 to 6 times lower than those used in this study. Riedel found that riparian plant roots contributed significantly to streambank stability. Removal of riparian vegetation by cattle grazing and hoof shear reduced the stability of streambanks below the thresholds for gravitational and fluvial erosion. Consequently, streams with grazed riparian areas had significantly widened; channels had enlarged, width depth ratios increased, and sinuosity decreased. Despite these morphological adjustments, the grazed streambanks, were significantly weaker than forested streambanks.

Riedel, Verry & Brooks (2002) employed comparative dendochronology of trees at varying stream terrace levels and other techniques to find multiple episodes of channel incision in the basin, attributed to timber harvesting in 1850, the Hinckley fire of 1894, and the Cloquet-Moose Lake fire in 1918.

Riedel, Verry & Brooks (2005) found strong correlations between land use and bankfull discharge, and between bankfull discharge and slump occurrence.

In another paper, Riedel, Verry & Brooks (2006) used the Pfannkuch and mechanisitic methods to study grazed riparian stretches along Deer Creek under a variety of cattle traffic scenarios over a three-year period. They concluded that stream bank stability was significantly reduced in grazed riparian areas. The empirically-based Pfannkuch stream bank stability index (PSI), a method of rating stream bank stability in the field, was consistent with mechanistic estimates and with measured values of stream bank stability.

Magner and Brooks (2007) used stream geomorphology metrics to predict stream channel erosion in the glacio-lacustrine clay deposits of the Nemadji River basin. The study concluded that the Nemadji River basin may likely remain in fluvial disequilibrium well into the 22nd century. The study did not take into account glacial isostatic rebound (see geology section following).

In June 2008, Andrew Streitz of the MPCA presented the results of a groundwater model for the Deer Creek TMDL project. One conclusion from his modeling stated that the sediment volcanoes occur in an area of thinner surficial clay. The model is expected to be refined to evaluate the effect of tree plantings and groundwater withdrawl on evapotranspiration and recharge.

A stable isotope study by Tom Schaub of the MPCA is currently in progress. The goal of the study is to use oxygen and hydrogen isotopes to determine the relative contributions of groundwater and precipitation to Deer Creek.

In July 2005, Mooers and Wattrus completed an investigation of groundwater seepage and excess turbidity in Deer Creek, which served as the basis of this study. The investigation included a history of the sediment volcanoes, glacial history, field investigation (including a seismic refraction survey), an analysis of the stratigraphy, and failure analysis along a cross-section of the Nemadji River basin.

Subsurface information from 34 water well borings from the Minnesota County Well Index was entered into 3-D modeling software and stratigraphic and potentiometric relationships determined. An analysis of slope failure potential was conducted along a cross-section near Deer Creek using the Mohr-Coulomb failure criterion to determine areas susceptible to failure by slumping.

Location

The Nemadji River basin covers approximately 433 square miles and is located southeast of Lake Superior, straddling the Minnesota-Wisconsin border (Figures 1 and 2). The watershed area includes much of eastern Carlton County, Minnesota, and extends into northeast Pine County, Minnesota, as well as northwestern Douglas County, Wisconsin. Approximately 300 square miles of the Nemadji river basin are in Minnesota. The maximum elevation in the Minnesota portion of the Nemadji basin is approximately 1360 feet, as shown on a 30-meter DEM of the study area (Figure 9). The mouth of the Nemadji River has an elevation of approximately 602 feet, resulting in a relief of approximately 760 feet. Red clay sediments comprise about 40% of the study area. The land cover is 69 percent boreal forest, 18 percent cropland and pasture, 11 percent wetlands and lakes, and two percent other categories (NRCS, 1998).

Approximately 80% of the Minnesota portion of the Nemadji River basin is located within Carlton County including all of the red clay erosion-prone areas and most of the headwater tributaries (Swenson, 2008). Additionally, electronic well data is only available for Minnesota wells. For these reasons, the study area for this investigation encompasses only the Minnesota portion of the Nemadji River watershed.

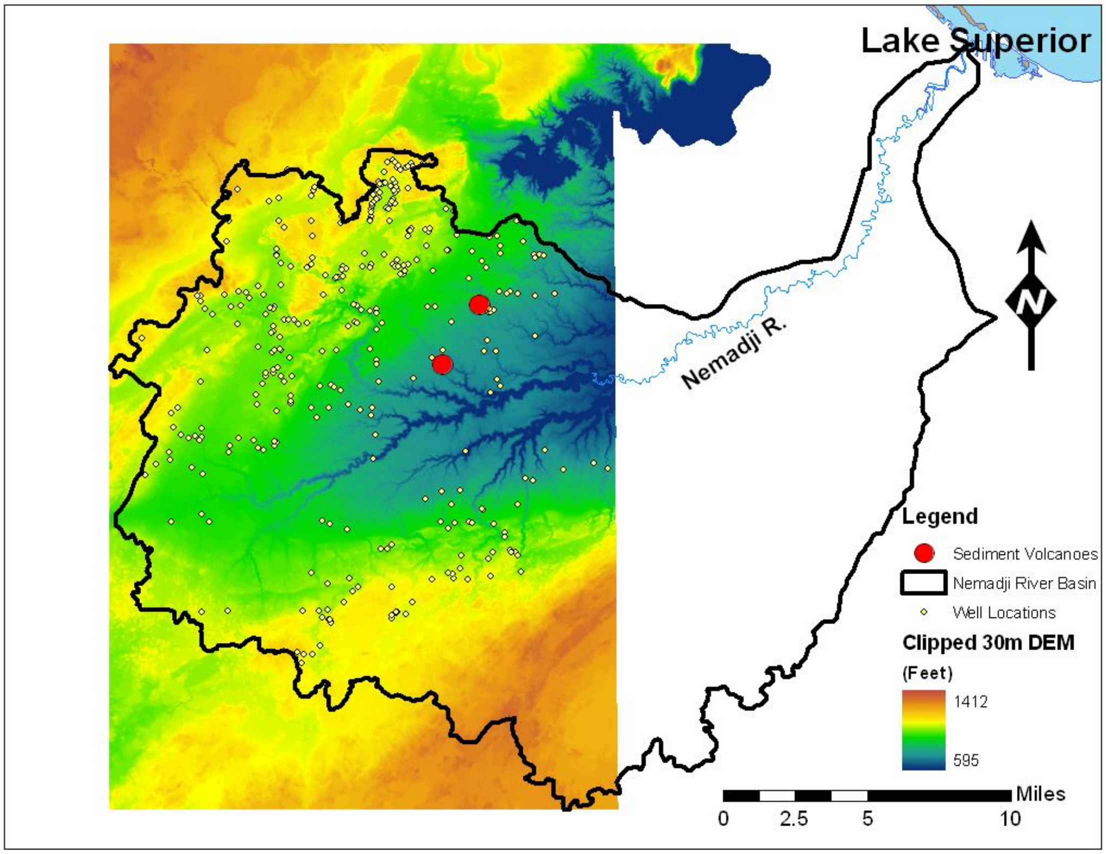

Figure 9. Digital elevation model showing well locations.

Geologic Setting

The general geology in the area of the Nemadji River basin is well known with numerous published maps, theses, and research articles. Winchell (1898) provided a description of the geology of Carlton County, and Leverett (1932) updated Winchell's work, describing the Quaternary history of the region. Wright, et al., (1964, 1972, 1973a & b) provided a detailed Quaternary history of glaciation in Minnesota. Farrand (1960, 1969, & 1985) studied the shorelines of former levels of glacial Lake Superior, and isostatic rebound of the earth's crust in the region after retreat of the glaciers.

The general sequence of glacial sediment in the area is known from regional investigations. Wright, et al., (1970) mapped and described the Cloquet Quadrangle in the northern part of the study site. Zarth (1977) mapped the geology of the Wrenshall and Frogner quadrangles which comprise much of the northern part of the study area of this project. Lannon (1986) examined the Quaternary stratigraphy and glacial history of the Duluth-Superior area. Carney (1996) studied the paleohydrology of the western outlets of glacial Lake Duluth. Maps were compiled of the regional geomorphology by Mooers (1996a & b). Johnson and Mooers (1998) described ice-margin positions. Knaeble and Hobbs (2009) provided detailed mapping and stratigraphy of the Quaternary geology of Carlton County, and Patterson and Knaeble (2002) mapped Pine County, immediately to the south. Glacial events in adjacent northwest Wisconsin have been studied in detail by Clayton (1984).

Based upon information from previous investigations in the area, the geology of the Nemadji River basin generally consists of up to 800 feet of glacial and glaciolacustrine Quaternary unconsolidated deposits filling a northeast-southwest oriented bedrock valley created by the Midcontinent Rift. The bedrock is comprised of Precambrian slate, basalt, and sandstone.

Bedrock Geology

Since the depth to bedrock is up to 800 feet in the center part of the basin - the main area of concern in this study - bedrock is considered a minor factor in the slope stability modeling. However, a brief description of the bedrock geology is included here, since preglacial topography helped control the distribution of sediments and the current topography in the Nemadji River basin. Few outcrops exist in the basin, even in river valleys, so its bedrock geology is mostly inferred from exploratory drillholes, water-well logs, and regional geophysical investigations.

The Nemadji River basin is underlain by three main bedrock types (Figure 10) roughly divided into thirds geographically from northwest to southeast (Booerboom, 2009). The bedrock types listed in that order are: 1) greywackes and slates of the Paleoproterozoic (approx 1900 Ma) Thomson Formation of the Animike Group; 2) sandstones of the Mesoproterozoic (about 1100 Ma) Fond Du Lac and Hinckley Formations; and 3) basalts of the Mesoproterozoic Chengwatana Group. The latter two bedrock types are associated with the Keweenawan Supergroup of the Midcontinent Rift, and have their contact along the Douglas Fault. The Midcontinent Rift forms a graben which provided a valley for later glacial lobes to travel down.

Depth to bedrock ranges from 0 feet at Thomson Formation outcrop exposures in the north side of the study area, and at Chengwatana basalt outcrops in river valleys in the south side of the study area, to more than 800 feet in the central parts of the basin (Knaeble and Hobbs, 2009).

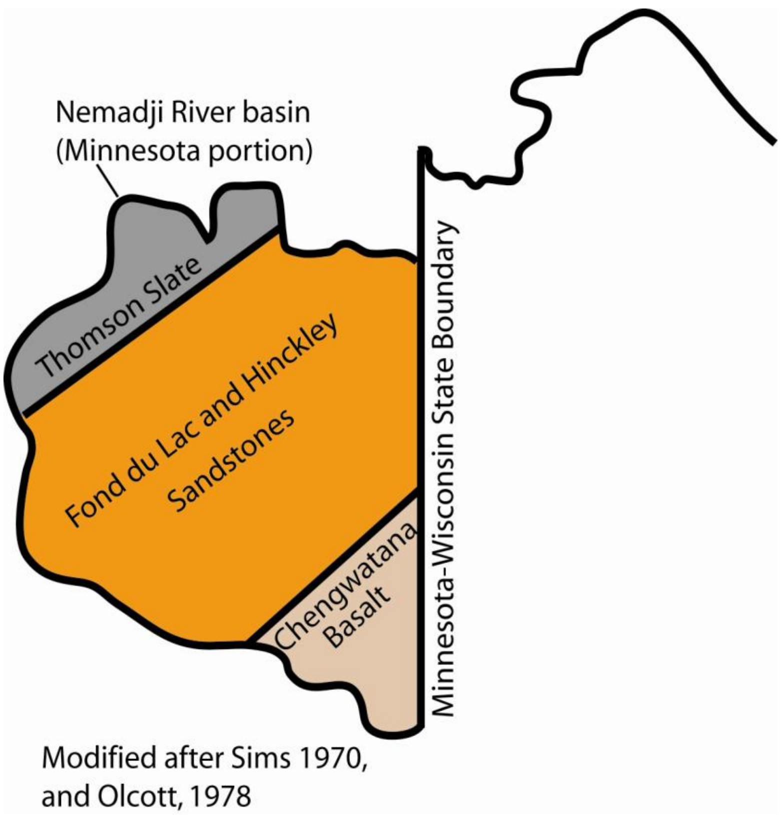

Figure 10. Bedrock geology of the Nemadji River Basin (Minnesota portion only).

Glacial Geology

The Nemadji River drains a broad lowland bound on the north, west, and south by hummocky topography of the Nickerson and Thomson glacial moraines (Figure 11). The lowland was formed by the Midcontinent Rift which provided a pathway for later continental glacial ice of the Superior Lobe of the Laurentide Ice Sheet and associated deposition of till, lake, and morainal sediments.

The study area has been glaciated multiple times in the past 2 million years by lobes from the Laurentide ice sheet emanating from the northeast. Evidence of earlier Pleistocene glacial stages (i.e., Illinoian, Kansan, and Nebraskan) were mostly wiped out by the last stage, the Wisconsinan stage, so little is known about glacial events in the Lake Superior Region prior to the Wisconsinan. However, a more complete record of glacial events is recorded in central Minnesota (Meyer, 1986, 1999, Mooers, 1988).

The Superior lobe advanced and retreated from its maximum limit numerous times, called "phases" (Wright, 1964, Wright et al., 1973). There are five major identified phases, each phase advancing less extensively to the southwest: the St. Croix, Automba, Split Rock, Nickerson, and Marquette phases.

Proglacial lakes formed in the study area between the retreating lobe and a distinct end moraine during several of these phases (Wright and Watts, 1969). The proglacial lakes allowed accumulation of fine grained lacustrine sediments in the deeper portions of the basin, and coarser-grained sediments at the beaches. The beach deposits include bars, spits, and deltas.

Ice likely retreated well into the Lake Superior basin because deposits of successive ice advances are rich in red clay. Clay only accumulates to appreciable thicknesses in large bodies of relatively still water (Wright, 1972). The reddish color was imparted from iron in the Midcontinent Rift parent rocks. The fine-grained sediments became entrained in the glacial till during readvances. Each successive readvancement ground up more fine material. The repeated process of fine-grained glacio-lacustrine sediments being thrust onto coarser beach deposits left massive alternating till and lacustrine clay units interfingered with sand. The sand fingers, forming at higher elevations of the lake stages, are often connected to the moraines (Mooers and Wattrus, 2005). The sand units at lower elevations in the basin are thus artesian aquifers, confined by clay.

The Nickerson Moraine is composed of clay-rich till and glacial lacustrine sediment and outwash (Figure 11). In contrast, the Thomson Moraine is composed mainly of glacial outwash composed predominantly of sand and gravel (Wright et al., 1970).

As ice retreated from the Nickerson and Thomson Moraines, Glacial Lake Nemadji was dammed between the retreating ice and the higher morainic topography (Winchell, 1904; Leverett, 1929; Carney, 1996). Lake Nemadji drained through the Portage Outlet (Figure 11) into the Kettle River. Well defined beaches mark the upper limit of this lake at 1150 feet with the main Lake Nemadji stage at 1100 feet. Once ice retreated from the Nickerson Moraine along the border between Minnesota and Wisconsin, Lake Nemadji coalesced with Lake Minong to the east, and the meltwater found a lower outlet along the course of the Brule River in Wisconsin (Clayton 1984, Carney 1996). The level of the lake dropped to 1065 feet and is marked by a prominent set of beaches in Carlton County (Figure 11). This stage of the lake is referred to as Glacial Lake Duluth.

The final glacial event was the readvance of the Superior Lobe at about 9900 years BP (Before Present) in an event known as the Marquette Phase. Ice likely advanced up to the inner margins of the Thomson and Nickerson Moraines (Hughes 1976, Clayton 1984). This event deposited a thick (30 to 120 feet) till on top of the previously deposited shallow water sediments of the previous lake phase.

As ice retreated for the last time Lakes Nemadji and Duluth again came into existence once again, although this lake phase was likely rather short lived. This event further complicated the stratigraphy depositing another clay rich, impermeable lacustrine unit on highly conductive shallow-water lacustrine sand.

Presently, red lake clays and silts, tills, beach sands, outwash sands, and gravels fill the Nemadji basin to a depth in excess of 800 feet. These deposits thin to less than 50 feet on the valley flanks in the northwest and southeast parts of the basin (Olcott, 1978). In the nearshore glacio-lacustrine environments of Lakes Nemadji and Duluth, thick sequences of sand were deposited (Mooers and Wattrus, 2005). These nearshore sands range from fine to coarse and onlap onto the gravel deposits of the Thomson Moraine. The deepwater sediment consists of fine silt and clay. Although the general relationship between the nearshore and offshore sediment is apparent, the details are not well constrained. Glacial advances into proglacial lakes reworked lacustrine clay, making it difficult to distinguish massive lacustrine clay from clay till.

Wright, et al., (1970) mapped the lacustrine red clay as the Wrenshall Formation, and described it as containing "some gray (oxidized yellow) silt, and red sand near former shoreline." The clayey till ground moraine and the lacustrine clay interbedded with silt, sand, & ice-rafted boulders from higher stages of glacial Lake Superior belongs to the Nickerson Moraine Association as mapped by Hobbs, 1982.

Knaeble and Hobbs (2009) classified the off-shore silt and clay lake deposits as the Wrenshall Member of the Barnum Formation. They described the Wrenshall Member as: "texture ranges from massive, almost pure clay, to alternating clay-rich and silt-rich laminated beds. Thin, very fine- and fine-grained sand layers occur locally. Clay layers are typically red but in places are dark gray. Silt layers are gray and may contain very fine-grained sand. Moderately to slightly calcareous. Pebbles and cobbles are rare, interpreted to be dropstones. Exposed by erosion on steep modern river slopes; tends to slump."

The base level for the Nemadji River was as low as 550 ft. above sea level (asl) during a Holocene dry period at 8000 b.p., which would have increased the gradient of the river, allowing more incision into the red clay (Farrand, 1985). The current base level, reached at about 5500 b.p. is approximately 602 feet. Post-glacial features are represented by deeply incised channels of up to 120 ft. (Zarth 1977). More recent floodplain stream sediments from the Nemadji River and tributaries may locally overlie the till and lacustrine red clay (Clayton, 1984)

Glacioisostatic rebound has been occurring in the area since the retreat of the glaciers. Currently the northeastern side of Lake Superior is rising at a rate of 27 cm per century, and the Nemadji area subsiding 21 cm per century relative to Lake Superior's outlet at Sault Ste. Marie (Farrand, 1985). The rebound has allowed water from the lake to transgress into the Duluth-Superior harbor, forming a drowned estuary.

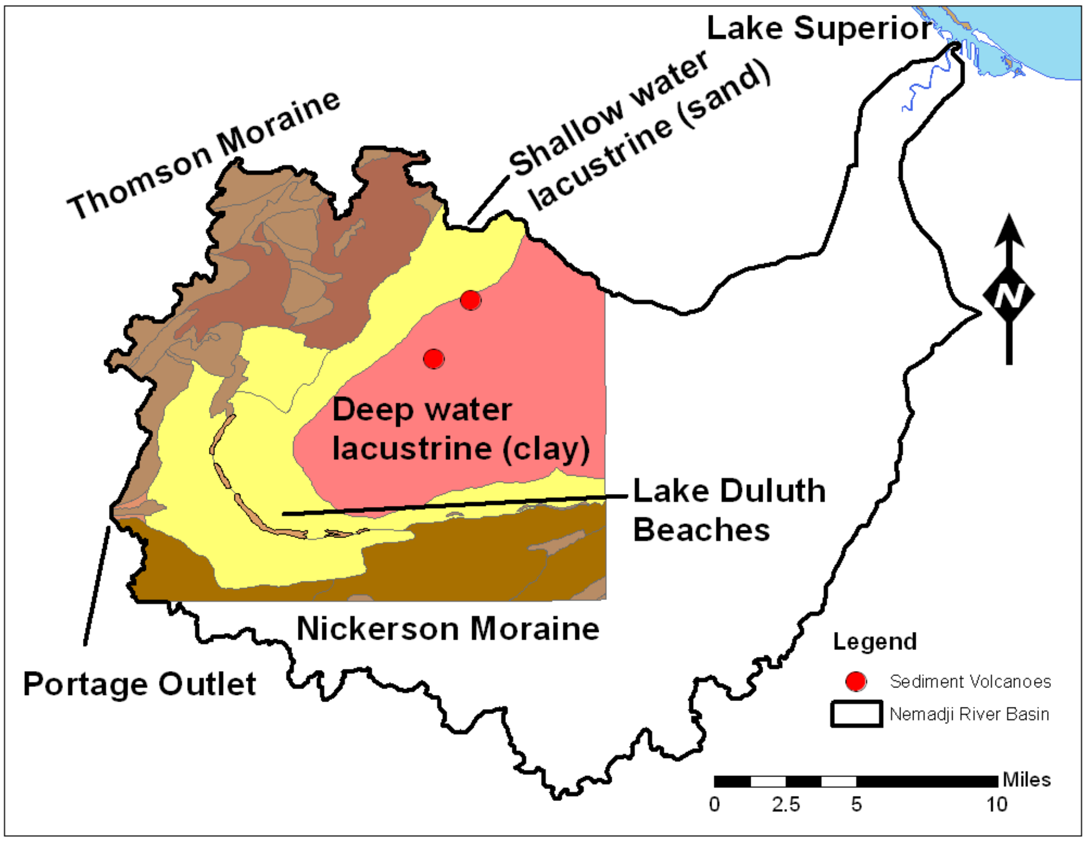

Figure 11. Glacial geology of Nemadji River Basin.

Hydrogeology

Depth to groundwater ranges from 285 feet around the perimeter of the basin, to artesian in the central parts of the basin (Olcott, 1978). Precipitation in the basin averages about 30 inches a year, with about 12 inches of runoff and 18 inches of evapotranspiration (Olcott, 1978).

Regionally, groundwater recharges downward through glacial drift near the margins of the basin down into bedrock, is semi-confined by lake clays, and discharges upwards near the rivers in the central parts of the basin under artesian conditions (Olcott, 1978).

Mooers and Wattrus (2005) illustrated that the sediments of the Nemadji River basin generally consist of a thick sequence of lacustrine clays and clay tills interbedded with thin nearshore lacustrine sediments composed of sand. These nearshore sands communicate hydraulically with coarse sand and gravel sequences in the topographically higher Thomson moraine. Potentiometric head in the confined lacustrine sands therefore reflect the elevation potential of groundwater in the moraine.

Mooers and Wattrus (2005) described two productive unconsolidated confined aquifers in the Deer Creek area. The uppermost of these shallow water lacustrine sequences lies at an elevation of 850 feet. The potentiometric surface in this aquifer lies roughly 100 feet above the top of the aquifer. The results of their geophysical survey confirm the stratigraphic observations from well borings, and furthermore divides the clay confining unit into essentially two layers there; an upper unit about 8 meters thick underlain by another unit about 34 meters in thickness. Analysis of the seismic refraction survey suggests that at least one fault with 3 meters of offset can be seen in the subsurface, although it does not yet have any surface expression (Mooers and Wattrus, 2005).

METHODOLOGY

The scope of this investigation included compilation of background information (previous section), development of a 3-D stratigraphic and groundwater potentiometric surface model in RockWorks™, development of a predictive slope failure model in ArcMap™, and correlation of aerial photos and field observations with the predictive model. The slope failure model results were compared to another slope stability model, SINMAP 2.0. A review of mass wasting theory and the methods used in this study follow. A review of applicable methods are included as Appendix A.

Mass Wasting Theory

Mass wasting is the downslope movement of rock, regolith, and soil, under the influence of gravity (Easterbrook, 1999). Slope failure occurs because gravitational stress exceeds the resisting strength of the slope material. Slopes may fail by creep, flowing, sliding, or failing. Mass wasting types are classified by the time scale at which they occur, fast or slow. Slow types of mass wasting include creep and solifluction, the downslope flow of saturated soil (Easterbrook, 1999). Rapid mass wasting includes rock falls, rock or debris slides, mud or debris flows, earthflows, and finally the type of mass wasting examined in this project, slumps.

Slumps involve a mass of soil or other material sliding downward along a plane or along a curved, usually concave-upward rotational slip surface with backward rotation of the land surface at the top of the failure (Easterbrook, 1999 p.75). The latter type is known as a rotational slump, and the formation of a crescent-shaped cliff or scarp at the top of the failure surface (Figure 12) often occurs. Water can collect at the land surface/scarp junction, and infiltrate and lubricate the failure surface. At the bottom (or toe) of the slump, earthflow, or flow of soil can occur. Cracks at the head scarp can drain water, killing vegetation. Manmade structures may become damaged if located near a slump. Slumps frequently form due to removal of the slope base, whether from natural or manmade processes. Stream erosion and road construction are common initiators for slumping through the removal of the slope's physical support.

The process of slumping of granular material can be analyzed by considering a block on an inclined plane (Easterbrook, 1999 p. 58) (Figure 13). The block can represent a mass of granular material or a single grain. Gravity acts downward on the block, and the total gravitational force can be resolved into normal (perpendicular to the plane) and shearing forces. These forces can be divided by the area upon which they act to find the normal and shear stresses (force per unit area). The shearing stress acts to move the block downward along the plane, i.e., slumping. The equation for applied shear stress (τ) is the stress-slope equation:

$$\tau = \rho g h Sin\theta, \quad \text{(eq. 1)}$$

where ρ is the density of overlying sediment (sediment and water), g the acceleration of gravity, h the height of the sediment column, and $Sin\theta$ is the sine of the slope in degrees.

Strength is the maximum resistance to stress at the point of failure or rupture. The most common types of strength are shear, tensile, and compressive (Easterbrook, 1999 p. 59). The shear strength of a granular material is given by its internal friction between grains and by cohesion. Cohesion is a physical property of a substance. It is shear strength resulting from the intermolecular attraction between like-molecules, including water, within a body or substance that acts to unite them. The Mohr-Coulomb equation for shear strength (*Str*) of granular material is given by:

$$Str = C_o + (\sigma_n - P)\tan\phi, \qquad \text{(eq. 2)}$$

where C_o is the cohesive strength, σ_n is the gravitational normal force on the boundary of the clay or underlying aquifer, P is the water pressure, and ϕ is the resisting force from the angle of internal friction of the clay (Terzaghi et al., 1996).

Slumping can occur where the shearing stress on a mass is greater than the shear strength of the resisting forces.

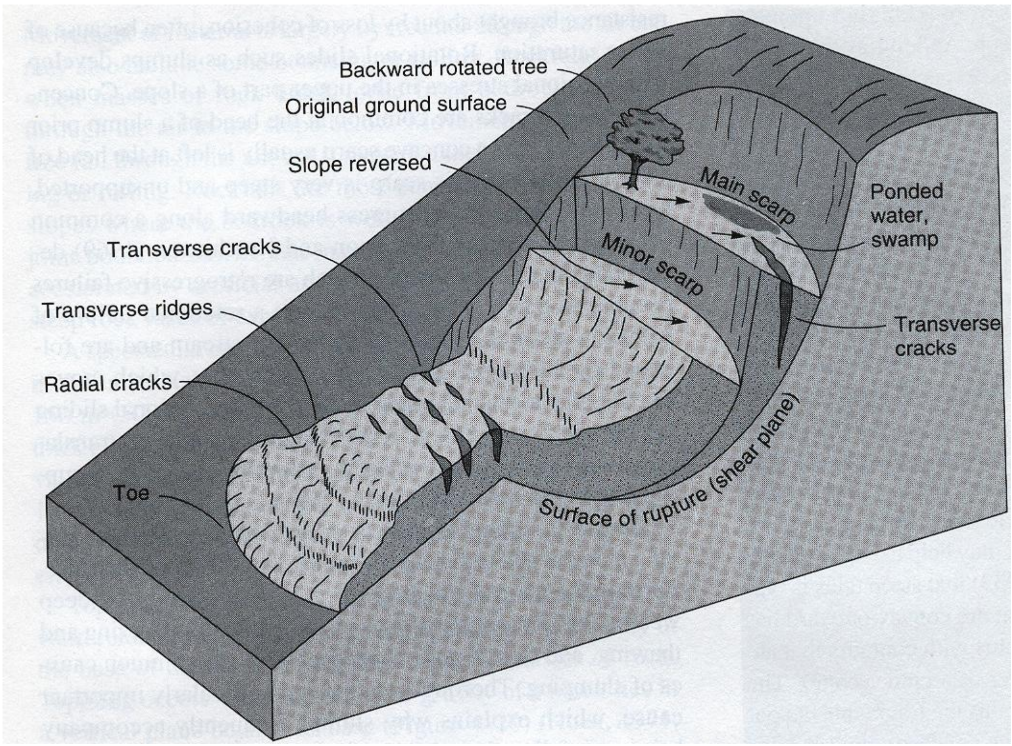

Figure 12. Rotational slump. From Easterbrooks, 1999.

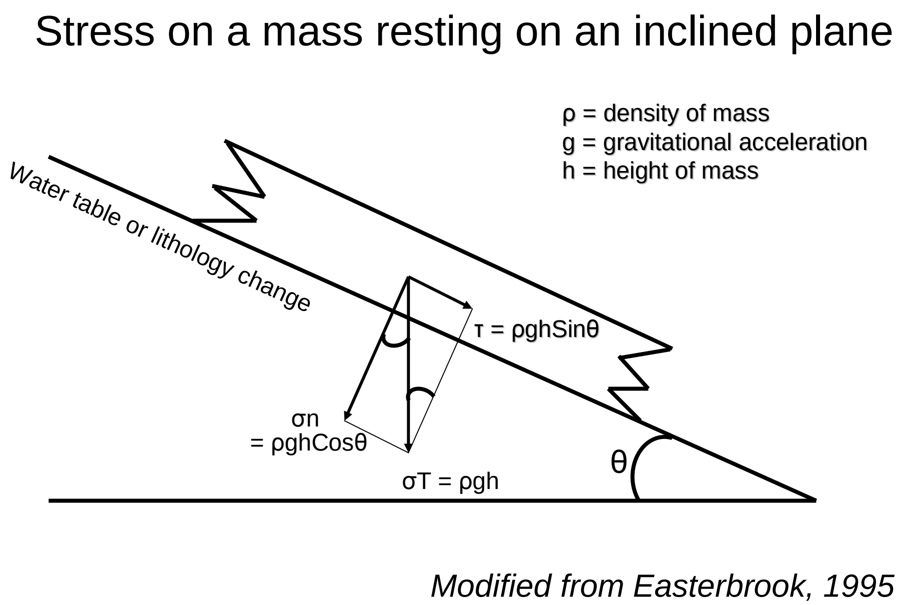

Figure 13. Diagram showing total (σT), normal (σn), and shear stress (τ) vectors.

Application of slope stability analysis in the Nemadji River Basin

Since most (98%) of the erosion in the Nemadji River basin occurs due to slumping (NRBP 2005), the method used here seeks to model the conditions in the Nemadji River basin that lead to slumping.

Slumps at Deer Creek are the result of failure of the clay confining layer along planes. In general, this type of failure results from excess pore water pressure reducing the shear strength of the material to below the driving shear stress. Slope stability can be determined by the interaction of hydraulic head (P) in aquifers, which serves to makes slopes unstable, with surface topography (Sinθ), since gravity acting on the slope of the land is the driving force causing failure.

While many methods or models use the infinite slope method, they disregard cohesion, which is an important factor in the stability of clay such as is found in the Nemadji River Basin. Riedel (2000) noted that the Mohr-Coloumb theory was developed for unvegetated slopes and will underestimate the strength of riparian streambanks. However, many of the Nemadji River basin streams are deeply incised into steep-walled clay bluffs, so much of the erosion is undermining or under-cutting banks with little vegetation (Figure 3). Additionally, the root system is generally above the failure plane and therefore cohesion due to vegetation does not appear to inhibit erosion and so is likely not a large factor in the calculations. Roots may merely serve to slow down the rate of slumping. Ignoring cohesion due to vegetation is also a more conservative approach. Vegetation adds weight to slopes and increases the shear stress, but can also reduce soil moisture (Easterbrook, 1999). However in areas of strong positive porewater pressure in artesian areas of the basin, theoretically more water would be supplied to soil moisture than vegetation could uptake.

The variability and complexity inherent in modeling slope stability implies that the straightforward application of the Mohr-Coloumb and stress-slope equations is appropriate for this study. Therefore, to examine the effect of changes in slope and hydraulic head on the potential failure of the clay confining layer the Mohr-Coulomb equation for shear strength and the stress-slope equation for shear stress will be applied across the Minnesota portion of the Nemadji River basin in a GIS (ArcMap™ v.9.2) for this project.

Site stratigraphy and hydraulic potential modeling

To assess the subsurface geology of the Nemadji River basin and form the basis for regional slope stability analysis, a 3-D stratigraphic model was developed using information from well driller's logs from the County Well Index (CWI). The CWI is a computerized database maintained by and available from the Minnesota Geological Survey (MGS) and the Minnesota Department of Health (MDH). The well logs include well locations, elevations, stratigraphy and water level data.

Only wells that were located and digitized by the MGS and/or MDH were used (i.e., the "cwilocs" file). These wells represent only about one-third of the wells in the

CWI database, but include wells that have geologically interpreted logs and aquifer determinations. The following steps describe the process used for downloading, filtering, and importing well information into the stratigraphic model:

1) A GIS shapefile (called "wells.shp"), which contains the located well information for the State of Minnesota was opened from the cwilocs file in ArcMap.
2) Next, another shapefile containing the areal extent of the Nemadji River watershed was obtained from the MnDNR's on-line "Data Deli," an internet-based spatial data acquisition site.
3) The Nemadji shapefile was dissolved to combine sub-watersheds into a single watershed, and then rasterized using ArcToolbox™. This rasterized watershed file was used to clip the wells in the Nemadji River watershed out of the statewide "wells.shp" file.
4) Next, the attribute table of the Nemadji wells shapefile was exported into a database. This was done so that stratigraphy data from a separate database table from the CWI called "C4ST" could be appended to each well. The resulting database included the location, elevation, stratigraphic information, and static water levels from the logs.
5) The database was then exported to a spreadsheet so that it could be imported into RockWorks®, a comprehensive geological database and graphic display system.

The stratigraphic descriptions from the well logs were simplified to allow units with similar properties to be compared for subsurface analysis. Well logs were plotted as cross-sections and 3-D block diagrams to develop a conceptual model of regional stratigraphy and groundwater systems. The model menu summary, which includes specifications such as spacing and interpolation method, are presented in Appendix B.

Aerial photos, topography (digital elevation models), and cultural features (roads, etc.) were overlain onto the 3-D images to aid in geological interpretation.

A potentiometric map of hydraulic head was created and added to the 3-D display of stratigraphic data, and it was also exported to the GIS for use in the slope stability analysis.

Failure analysis method

The objective of the failure analysis is to develop a map showing areas in the watershed susceptible to failure. The overall conceptual framework for this portion of the project is to generate raster grids of shear stress and shear strength in the Nemadji River watershed. These grids are compared with (subtracted from) each other to produce another raster grid showing where the stress exceeds strength, an indication of higher susceptibility of failure of the overlying clay layer and thus potential for slumping and sediment volcano formation.

To accomplish this task, data were compiled and processed in the following manner:

1) The 30-meter Digital Elevation Model (DEM) raster for Duluth was downloaded from the MnDNR Data Deli. A shapefile containing the areal extent of the Nemadji River watershed was obtained from the same source.
2) The boundaries of the subwatersheds in the shapefile were dissolved to combine them into a single watershed, and the resulting shapefile was rasterized using ArcToolbox™.
3) This rasterized watershed was used to clip the DEM down to the size of the Nemadji River basin.
4) The clipped DEM was used to produce a slope raster (in degrees) using the Spatial Analyst™ tool.

The applied shear stress was calculated with a raster calculator using the slope-stress equation (eq. 1, p. 29). The following values in Table 1 were used:

Table 1. Shear Stress values used in the slope-stress equation, $\tau = \rho g h \sin\theta$.

Parameter	**Value**	**Comments**
ρ(sediment)	1670 kg/m^3	laboratory measurement of samples from study area
g	10 m/s^2	constant
h	10 m	from field observations
θ	0 to 90 degrees	raster slope in degrees from DEM

Mooers and Wattrus (2005) used a density value for clay of 1325 kg/m^3 assuming 50% porosity in their failure analysis. Terzaghi (1996) indicates a wide range of clay density values typical of soil in their natural state at varying porosity and water contents. Those values range from 1270 to 2310 kg/m^3. Since a wide range of values were encountered, a simple laboratory measurement of the density of clay in the Nemadji River basin was conducted.

Three clay samples were collected from the study area for density analysis. The first sample was collected from a hillside slope of the Nemadji River, approximately 50 feet above the river elevation. The second sample was collected from a nearby cut-bank on the river. The third sample was from an exposed slump scarp at the Deer Creek pond area. A shovel was used to dig approximately 1-foot into the ground at each site to obtain the sample. Care was taken to minimize disturbance of the samples. The samples were taken to a laboratory the same day, and individually weighed on an analytical balance. The samples were then each placed in a graduated cylinder partially full of water to measure the displacement volume. The mass of each sample was divided by its volume to obtain density. The results of the three samples were 1670, 1660, and 1630 kg/m^3, respectively. The 1670 value was used, since the first sample was obtained from the least disturbed in-situ condition.

Since site stratigraphic modeling did not identify a clear failure plane, the heights of the probable failure planes at Deer and Mud Creeks were used for the height values in the stress and strength calculations. The maximum possible failure plane depth was taken as the maximum relief between the creek bed, where the sediment volcanoes occur, and the top of the creek bank, where the top of the slumps are located. The failure plane was identified using the 'Create Profile Graph' feature in ArcView™ 3DAnalyst (Figure 14), and resulted in a height of approximately 10 meters in each case. This height was used for (h) in the stress-slope equation, and to calculate the normal force in the Mohr-Coloumb equation.

A raster calculation was performed using the Mohr-Coulomb equation for shear strength of granular material (eq. 2, p. 29). Textbook values for clay cohesion range from 5000 to 50,000 N/m^2 (or Pa) (Terzaghi et al., 1996). The unconfined compressive strength of clay in the area is typically 1,000 to 2,000 pounds per square foot (psf), or approximately 47,000 to 95,000 Pa (Gary Hage, P.E., personal communication).

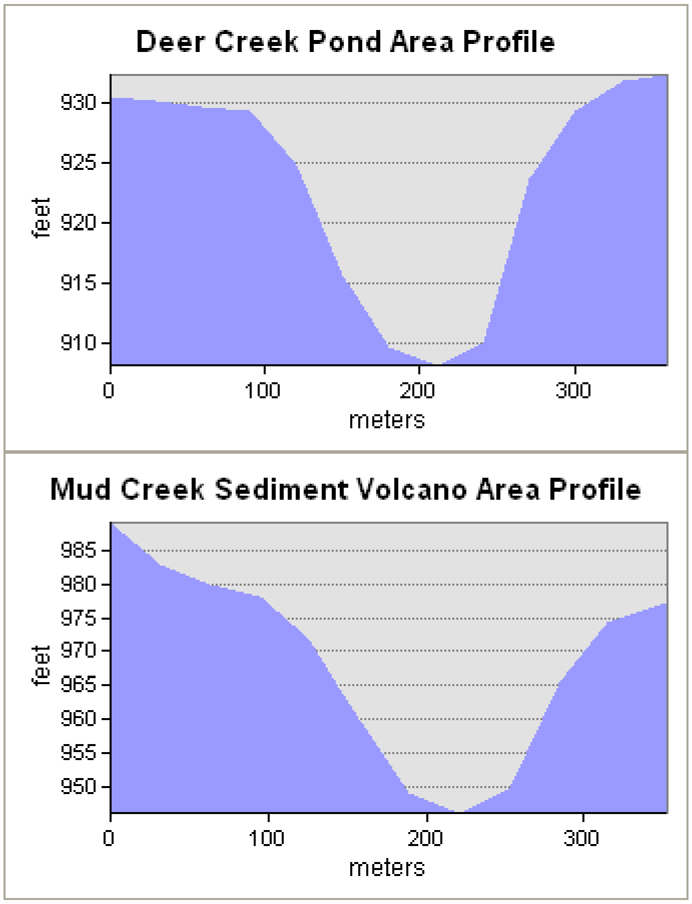

Figure 14. Deer and Mud Creek elevation profiles.

Since a wide range of cohesion values are possible, a value of 25,000 Pa was used as a conservative estimate. The normal stress was calculated using a height of 10 meters, the observed height of a typical failure plane. The density of the clay was taken as 1670 kg/m^3 as measured in the laboratory. Water pressure, P is equal to ρghn, where ρ = 1000 kg/m^3 for water, g = 10 m/s^2, and n (porosity) = 0.5 (Terzaghi et al, p.22). The height, h, was determined by the height of the potentiometric surface map generated in RockWorks® above the 10-meter failure plane. The water pressure was set to zero where the water table was deeper than the 10-meter failure plane, by reclassifying the values in ArcView™ Spatial Analyst. The angle of internal friction of the clay, ϕ, is often similar to the angle of repose (Terzaghi et al., 1996 p. 104), and was averaged at 25° (Terzaghi et al., 1996 p. 154). A summary of the values used in the Mohr-Coulomb equation (eq. 2, p. 29) is presented in Table 2:

Table 2. Shear Strength values used in the Mohr-Coulomb equation for shear strength (Str) = Co + (σ_n – P)tan φ.

Parameter	**Value**	**Comments**
C_o	25,000 Pa	Terzaghi, 1996, p. 154
σ_n	ρ(sediment)gh|cosθ|	ρ(sediment) = 1670 kg/m^3, constant g = 10m/s^2, constant h= 10m, height of failure plane. |cosθ| = absolute value of cosine of slope
P	ρ(water)gh(water)n	ρ(water) = 1000kg/m^3, constant g = 10m/s^2, constant h(water) = Height of potentiometric surface. Negative where artesian, to a maximum depth of 10m (failure plane). n = Porosity (assumed 50%); Terzaghi, 1996, p. 22
Φ	25 degrees	Terzaghi, 1996, p. 154

A final raster calculation was performed using spatial analyst, subtracting the strength raster from the stress raster. Where the value of the shear stress was higher than the shear strength, a higher susceptibility for failure occurs. Non-clay areas were clipped out using a shapefile of the Nemadji River basin clay area provided by the CCSWCD, based on Bacig, 1993. A 60m buffer was applied to the succeptible areas to smooth out the results, and to provide a factor of safety. This should be reasonable considering a 30-meter DEM was used.

Sensitivity of the equations was inspected to determine which variables were the most significant; the effect of changing the values of those variables on the results was examined. Due to the complexity of the equations, there are many possible variable combinations. For example, if the height value in the shear stress equation is changed, then it must be changed in the normal stress component of the shear strength equation as well. Therefore, subjectivity in picking from a range of values based on observed field conditions was employed (e.g., picking a high cohesion value for "fat" lacustrine clay) as well as choosing conservative values where deemed appropriate. The effect of changing density and cohesion values was analyzed, however, and is discussed in the results section.

Correlation

The failure analysis model was correlated with field observations by comparing the model with two data sets of inventoried slumps, one from an erosion survey by the MnDNR 2000/2001, and the other from the master's thesis by Wold (1994). The MnDNR set consisted of 185 slumps mapped from helicopter along the main stem of the Minnesota portion of the Nemadji River. Wold employed aerial photography and field-verification to inventory 137 slumps in nine tributary subwatersheds of the Minnesota portion of the Nemadji River basin. Combining the data sets resulted in 322 slumps along the main stem and tributaries of the Nemadji River. Neither data set was available in electronic format, so both data sets were digitized by hand in ArcMap™.

Prior to performing the failure analysis, so not to influence results, Google™ Earth was used to investigate the Nemadji River basin from an aerial view for the presence of slumps. An "electronic marker" was placed at each suspected slump location. Approximately forty (40) slumps were identified. The markers were downloaded into a Global Positioning System (GPS) device using the software program DNR Garmin so that the slumps could be found in the field and checked. Only ten (10) were field-checked. Reconnaissance level investigation was done by walking along select streams within the Nemadji River basin. Digital photos and field notes were taken to document field work. Not enough suspected slumps were checked to draw any conclusions, but the exercise improved the author's familiarity with the terrain.

Limitations, Assumptions

The stratigraphy and water table elevation data used to build the 3D lithologic model are based on driller's logs. Well driller's logs are generally considered low-quality data. Although wells are concentrated in populous areas and not spread evenly throughout the basin, their abundance can be valuable in subsurface investigations. For this project, 334 wells were found in the approximately 300 square mile study area, an average of about 1.1 wells per square mile. The potentiometric surface generated by the modeling program was reconstructed from static water levels recorded at the time the wells were drilled. Although the water levels were recorded at different times, and in many cases different aquifers, the surface should still present a reasonable overall representation of hydraulic potential.

The geologic descriptions of the unconsolidated (glacio-lacustrine) deposits were simplified to facilitate interpretation. The stratigraphic modeling used a 50-foot (16.667 meter) vertical and horizontal spacing. Much geologic variation can occur over such a large area. The areal resolution of the 30-meter DEM is relatively low in comparison to the area and height of many slumps (5-30 meters typically). High angle slopes at smaller spatial scales become smoothed out by the DEM.

The equations used in the failure analysis provide a simplified representation of actual field conditions. For example, the Mohr-Coulomb equation doesn't take into account overconsolidation or freeze-thaw effects on bank stability. A shear failure is conventionally considered to occur along a discrete surface and is so assumed in stability analyses, although the shear movements may in fact occur across a zone of appreciable thickness (USACE, 2003) where strain and deformation may occur. Single cohesion and density values were selected for clay; however the actual values can change as the moisture content of clay changes. The model also doesn't take into account changes in the potentiometric surface that naturally occur.

Slump identification in aerial photos is somewhat subjective, and many slumps may be hidden in shadow, or by vegetation, or not encountered. Slumps are identified differently in the field than from aerial photos or helicopter because of the difference in perspective. The Wold slumps are over 25 square feet (8.333 meters) in size. The number and location of slumps was critical to his results as this information was used as the dependent variable in a regression analysis.

Comparison to another model

In consideration of the limitations and assumptions of the failure succeptibility analysis, another model was used to test the reliability of the failure analysis results. The model chosen was SINMAP 2.0 (stability index mapping), developed for shallow translational landslides (Pack, 1999). The SINMAP model was chosen because it provides a contrast to some of the main assumptions in the failure analysis used for this project (Appendix B). This model uses the infinite plane slope stability model developed by Montgomery and Dietrich (1994), coupled with steady state topographic hydrologic models rather than the standard Mohr-Coloumb method. In addition SINMAP allows for cohesion contributed by vegetation and roots, a factor ignored in the failure analysis conducted for this project.

The governing equation used in SINMAP to calculate the factor of safety, (FoS) is:

$$FoS = \frac{C+\cos\theta[1-\min(R*a/T\sin\theta,1)r]\tan\varphi}{\text{Sin}\theta} \qquad \text{(eq. 3)}$$

where C is a dimensionless combined root and soil cohesion factor relative to the perpendicular soil thickness and density. This may be thought of as the ratio of the cohesive strength relative to the weight of the soil, or the relative contribution to slope stability of the cohesive forces. Theta (θ) is slope angle, R is recharge, a is the specific catchment area of shallow subsurface flow along topographic gradients (i.e., contributing flow area divided by unit contour length), T is transmissivity, r is the water to soil density ratio, and φ the internal friction angle of the soil.

Default input values were used for some variables, such as 9.81 m/s^2 for gravity, since they were similar to the values used in the failure analysis performed in this project, and others were modified, such as 1670 kg/m^3 for density, since they were more representative of site conditions.

RESULTS

Results of stratigraphic and potentiometric modeling are presented followed by the results of the failure analysis, and correlation.

Site Stratigraphy and Hydraulic Potential Modeling

Within the defined study area, 334 wells were identified that had stratigraphic logs (Figure 9). Of these, 42 were located in the red clay area.

A block diagram showing the results of the 3D lithologic modeling was generated in RockWorks. Figure 15 is a cross-section of the model with section location map, from the northern edge to the center of the Nemadji River basin. The modeling generally agrees with prior geologic investigations, and shows the Thomson Moraine, composed primarily of sand with gravel and interbedded till sequences, and the Lake Duluth basin, composed mainly of clayey till and glacio-lacustrine clay with interbedded sand and gravel units. The model also shows bedrock as described earlier. The model illustrates the complexly interbedded sand, gravel, and till of the moraine in contrast to the thin layers of coarse sediment within the clayey tills and lacustrine clays of the deep basin.

As illustrated in Figure 15, it is likely that the thin silts and sands in the deep basin are hydraulically connected to the sand and gravel of the Thomson Moraine. The complex lithology across the basin made it difficult to use the model for selection of a distinct failure plane, so field observations were used as noted in the methods section. A model of porewater pressure converted from the potentiometric surface above the theoretical 10 meter deep failure plane is presented in Figure 16. Some parallelogram-shaped relicts are visible in the figure as a result of the water table model nodes.

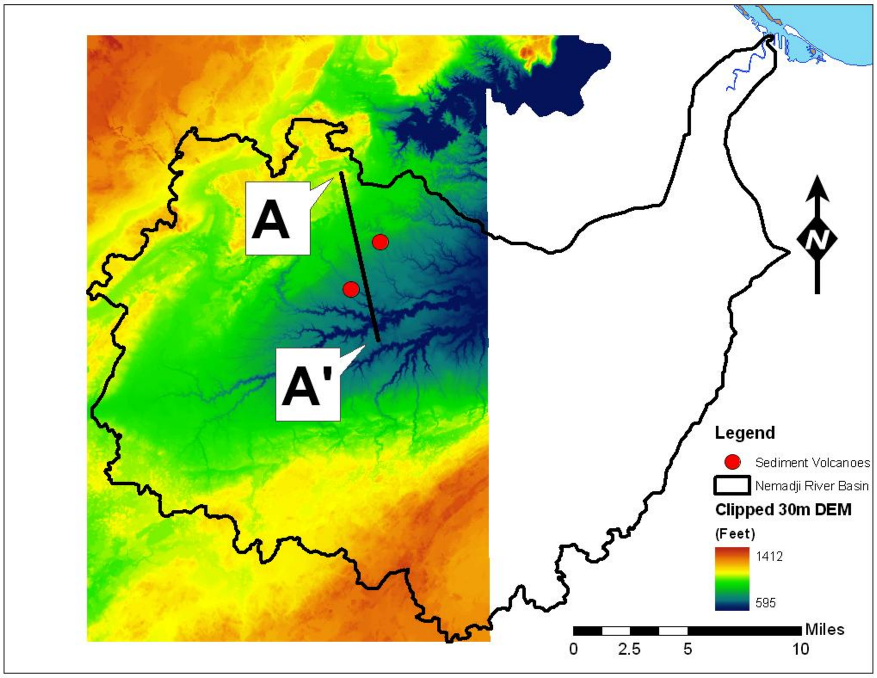

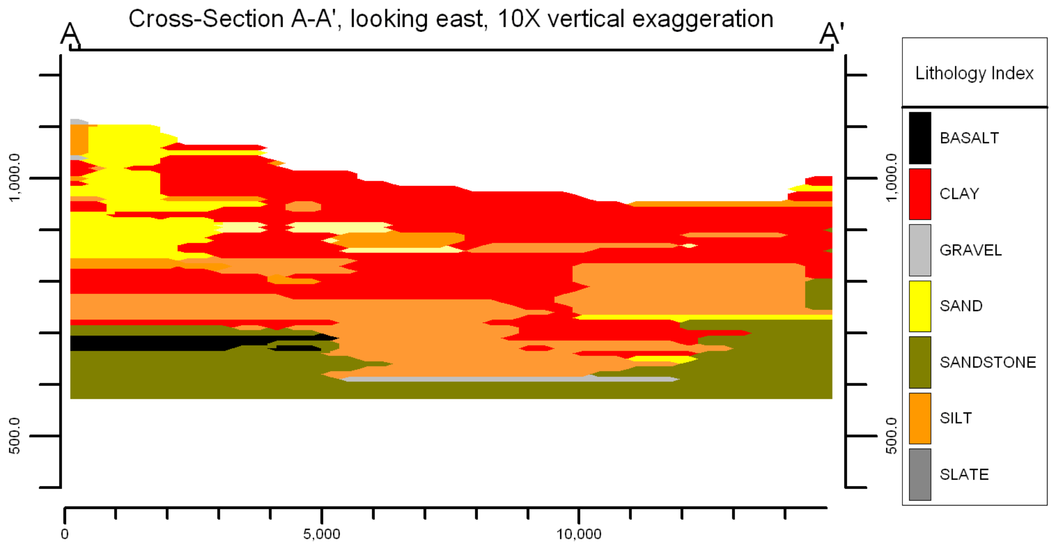

Figure 15. Cross-section location map and cross-section of lithology. Elevation in feet, horizontal distance in meters. See Figure 9 for locations of wells near the cross-section.

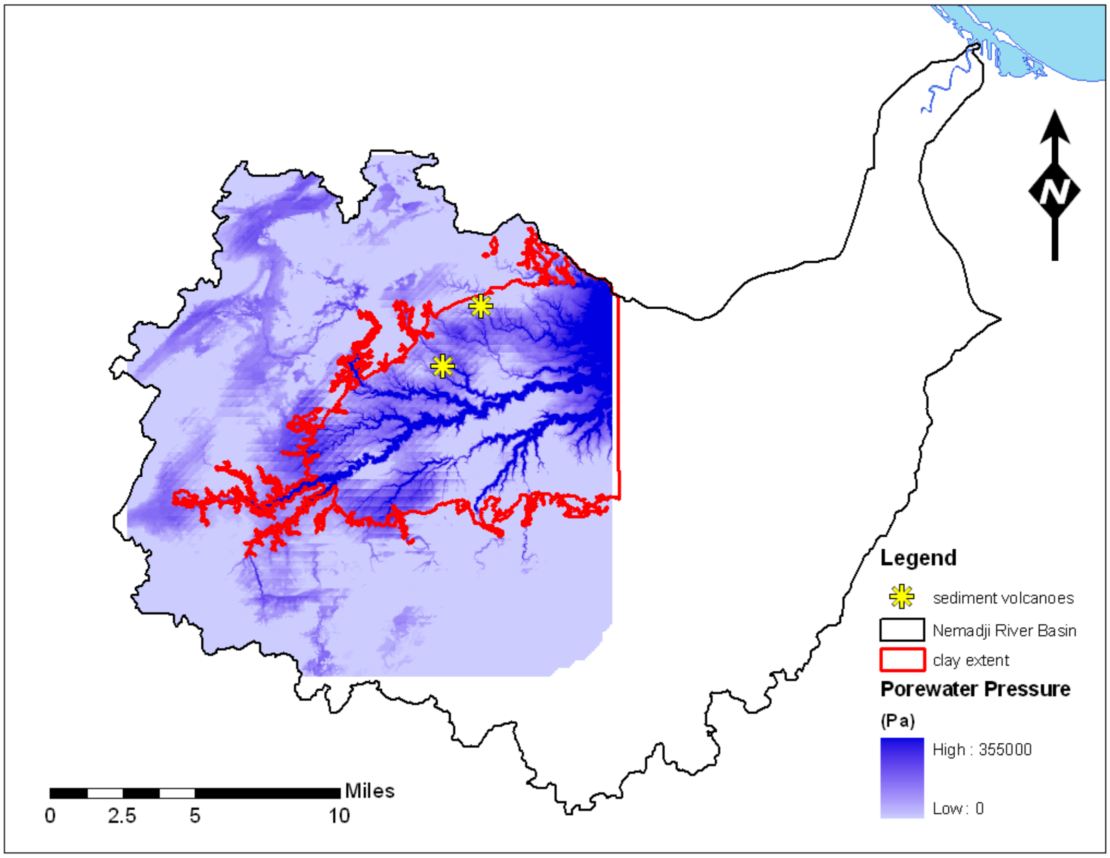

Figure 16. Map of porewater pressure above a theoretical 10 meter deep failure plane, converted from hydraulic potential.

Failure Analysis

Results of the failure analysis are presented in map form in Figures 17 through 22. The figures are components of and complete solutions of the stress-slope and Mohr-Coulomb equations, followed by results of the failure susceptibility analysis, and correlation of the analysis with previously mapped slumps.

Shown on Figure 17 is the slope of the land surface as generated from the DEM in ArcMap™, and Figure 18 displays the shear stress on the clay calculated from the stress-slope equation.

In Figure 19 the normal stress calculation result is presented, and Figure 20 displays the shear strength of the clay resulting from the Mohr-Coulomb equation. In some areas the shear strength is negative due to the high porewater pressure. As expected, the areas with the lowest strength are areas of increased slope and high hydraulic potential.

Finally, Figure 21 displays the failure susceptibility of the clay area; that is, areas where the shear stresses exceed the shear strength. Of the approximately 46,500 acres of the red clay area, 16,645, or 35%, were found to be succeptible to failure.

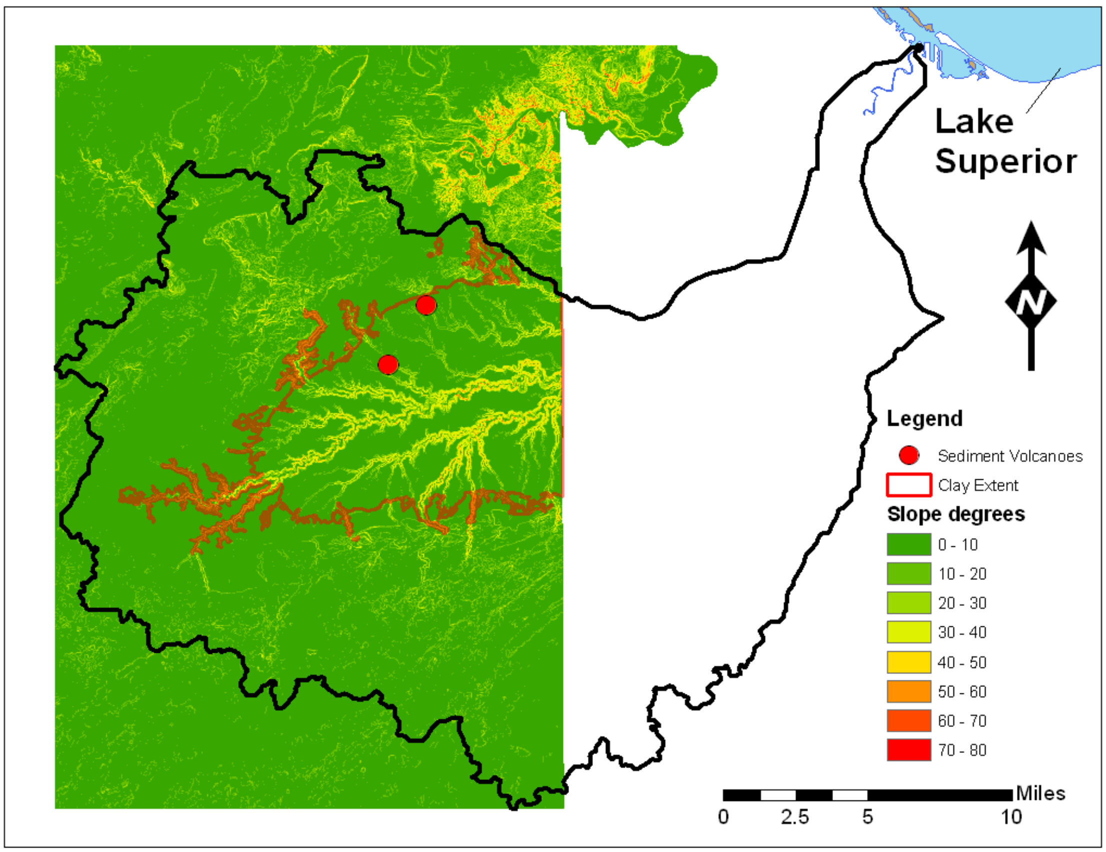

Figure 17. Topographical slope in the Nemadji River Basin.

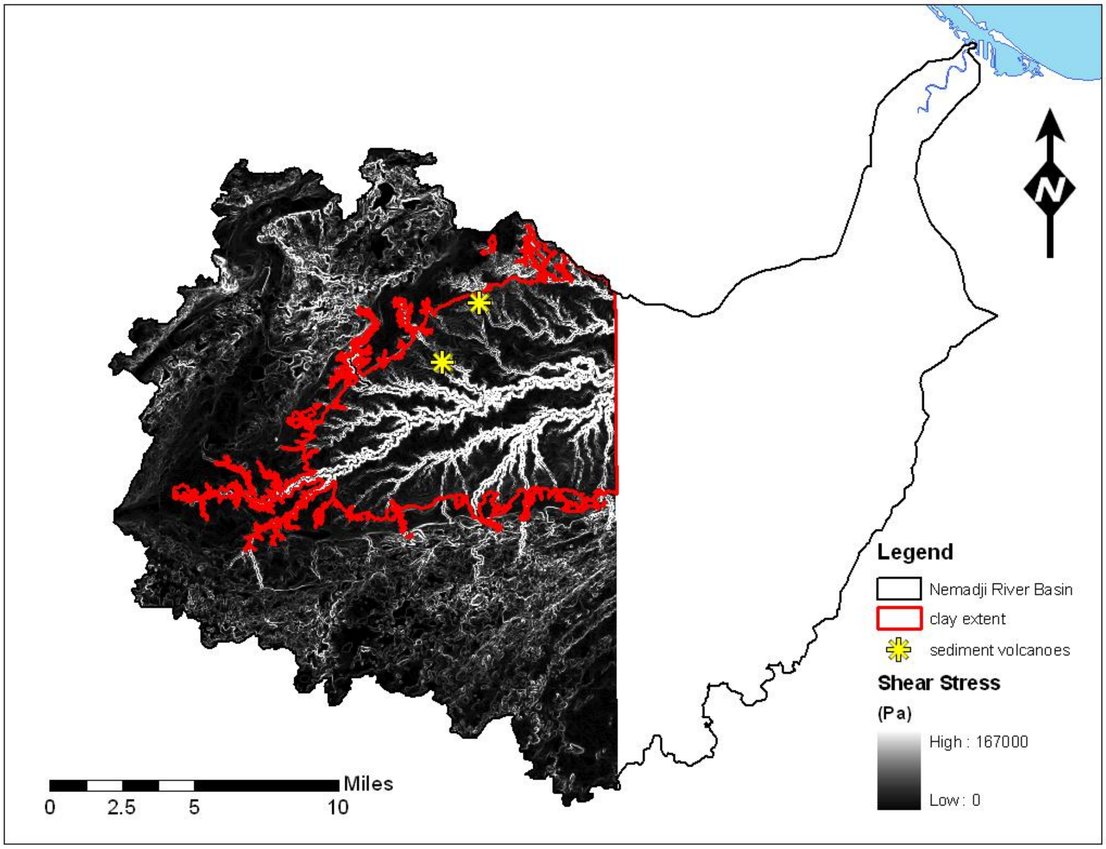

Figure 18. Shear stress.

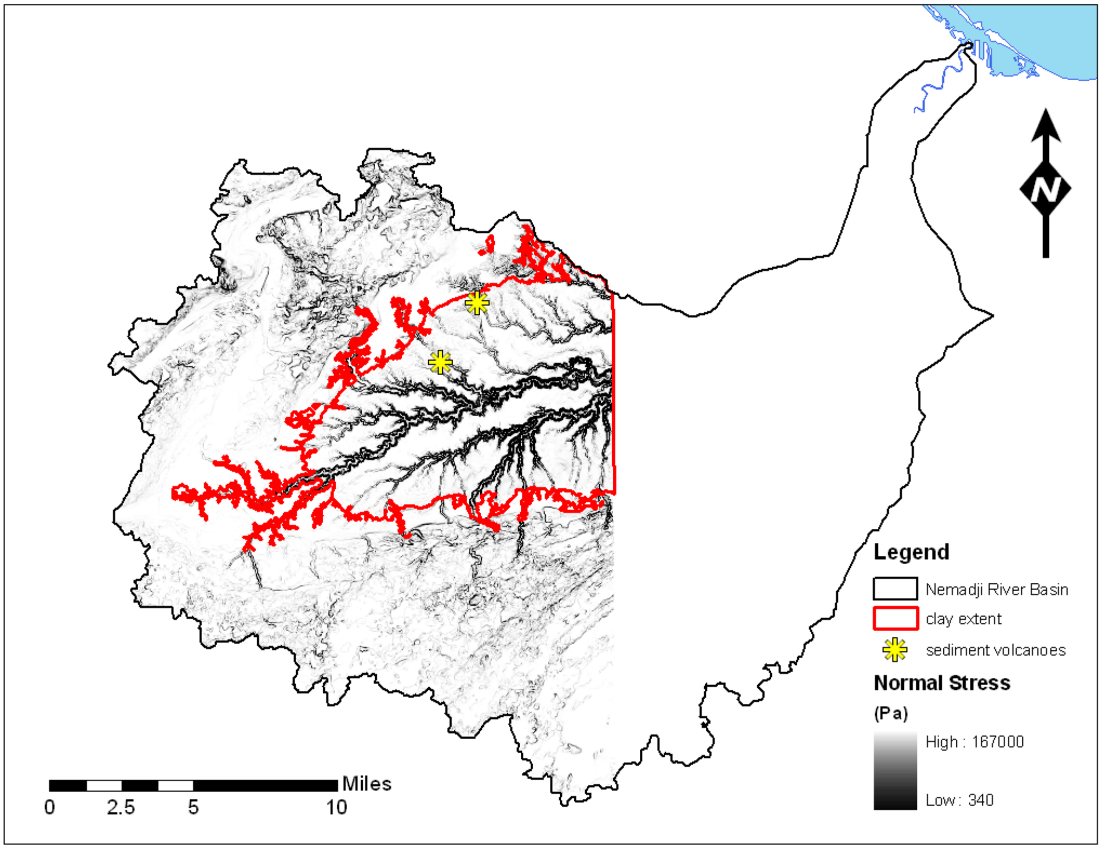

Figure 19. Normal Stress.

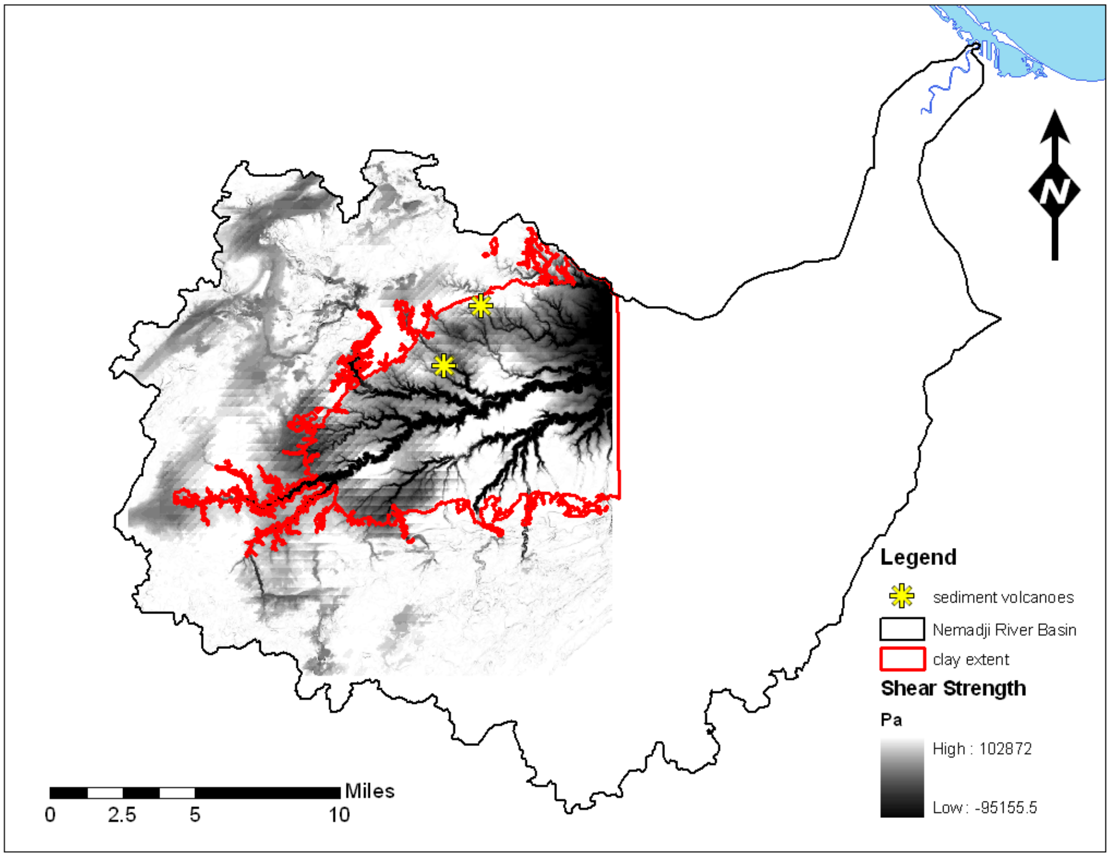

Figure 20. Shear strength using 25,000 Pascal value for cohesion.

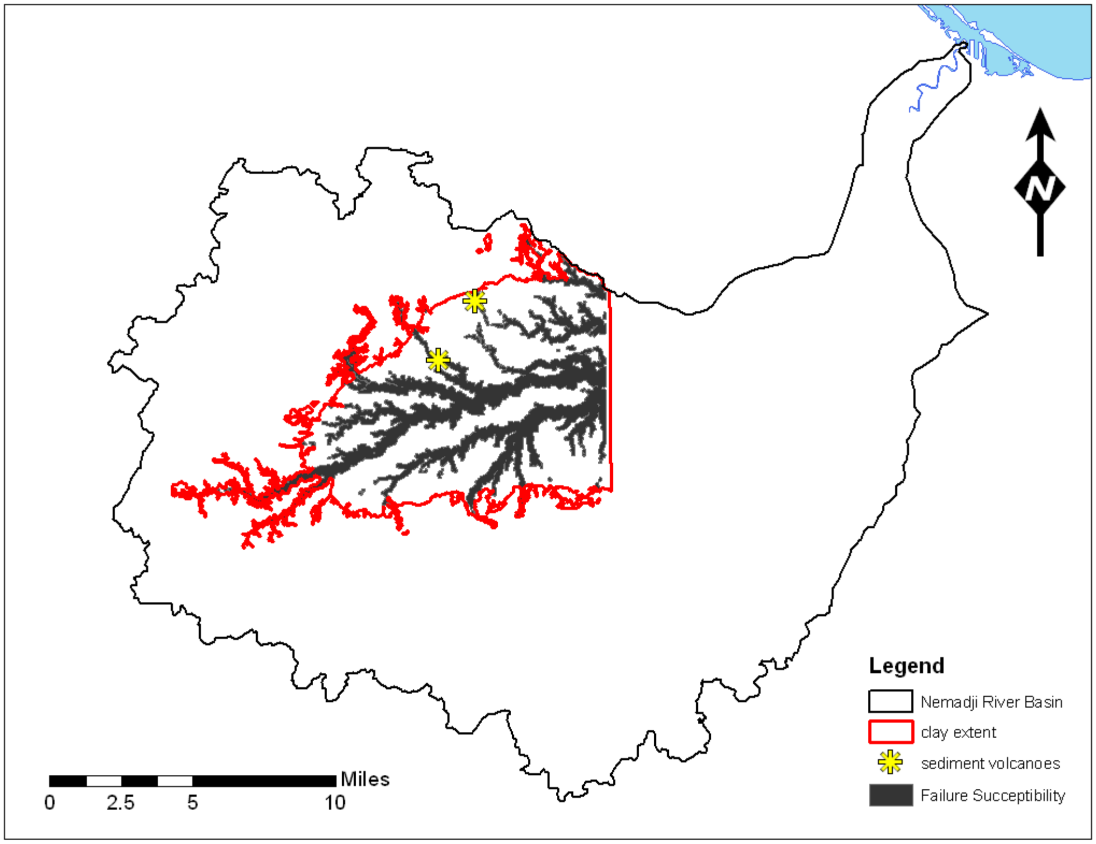

Figure 21. Failure succeptibility, with 60 meter buffer.

Examining the sensitivity of the stress-slope equation shows that shear stress sensitivity is rather straightforward. The variables can be considered invariant except for height, which can vary from 0 to 10 meters or possibly more depending on the height of a given stream bank. Since the DEM used for this study had a 30-meter horizontal resolution, it was decided that a height less than 1/3 of the resolution area (i.e., 10 meters) should not be used.

An analysis of the Mohr-Coloumb equation for shear strength shows that cohesion is the most sensitive variable, followed by the angle of internal friction, ϕ. A material such as sand, when dry and loose, can have essentially no cohesion. However, the geology in the area of concern consists mostly of lacustrine "fat" clay, so a somewhat high cohesion value was used, while maintaining a conservative estimate. The equation is also sensitive to the internal angle of friction. The range of possible values is 5-25 degrees (Terzaghi, 1996, p. 154). These translate into a value of 0.08 for the tangent of 5 degrees, and a value of 0.46 for the tangent of 25. The value of 25 degrees was used, since it reduces its side of the equation term by nearly half, lowering the shear strength, and therefore providing a more conservative result.

The effect of changing the density and cohesion values was analyzed. A clay density value of 2000 kg/m^3 yielded a shear strength value of 118,260 Pa; while a density of 1670 kg/m^3 yielded a shear strength of 102,872 Pa. However, since clay density is used in the shear stress equation also, those values change from a maximum of 200,000 Pa to 167,000 Pa.

The model was also run using a 75,000 Pa value for cohesion. Since this value resulted in a higher shear strength, the resulting failure susceptibility area was slightly smaller. The 25,000 Pa value was used for the final model because it provides a more conservative estimate.

Correlation

Figure 22 shows the Wold and DNR field-identified slumps plotted in relation to the predictive susceptibility model. Of those 322 slumps, 296 were within the model's predicted susceptible slump area, a correlation rate of 92 percent. The two sediment volcano areas at Deer Creek and Mud Creek were within the predicted susceptible area.

The results of the SINMAP 2.0 model showed a similar extent of failure succeptibility to the failure analysis conducted for this project (Figure 23). Of the approximately 46,500 acres of the red clay area, 13,458, or 29%, were found to be succeptible to failure (i.e., "quasi-stable" or less).

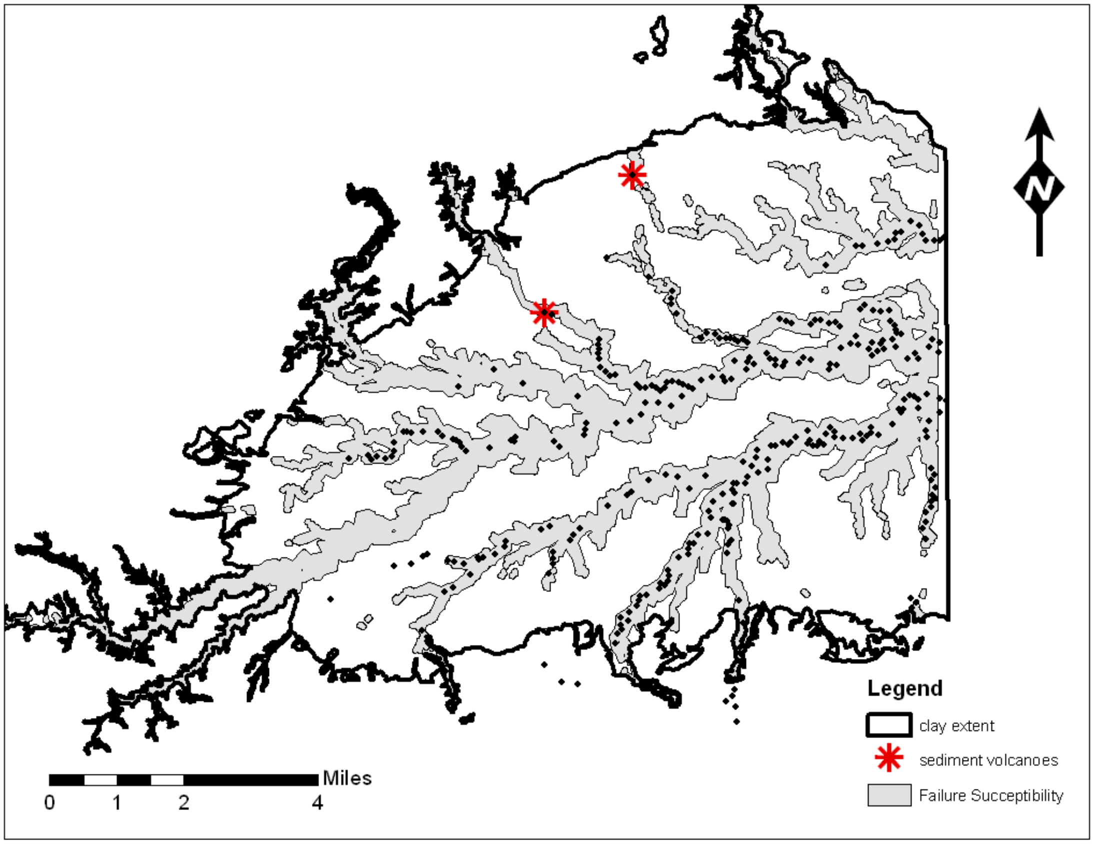

Figure 22. Correlation with Inventoried Slumps.

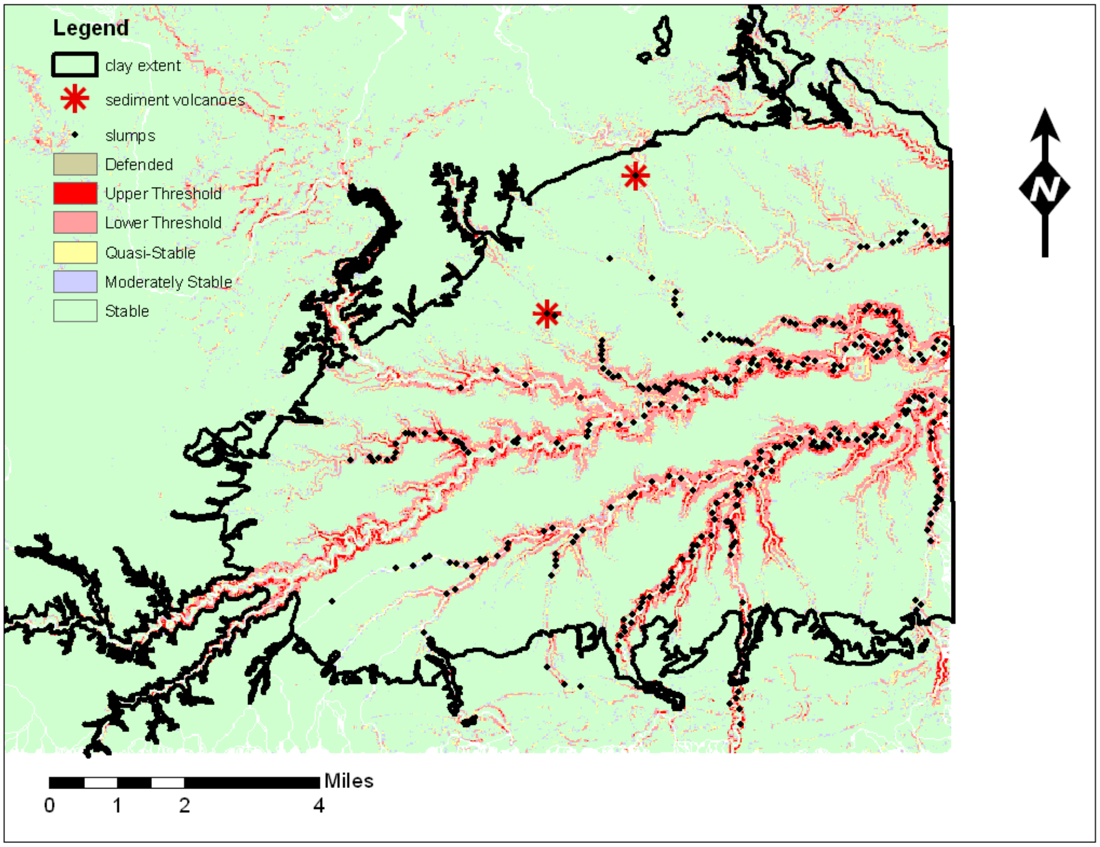

Figure 23. Results of SINMAP 2.0 modeling.

DISCUSSION

The Nemadji River basin has long been the major contributor of sediment to the Duluth-Superior Harbor and important Lake Superior fisheries. The problem of slope stability and turbidity is a major focus of several government agencies. Considerable time and monies have been spent trying to mitigate the effects of this excess sediment. Part of the reason for the ineffectiveness of the mitigation has been that the location and processes by which slope failure occurs in the Nemadji River watershed were poorly understood.

The recent studies of Mooers and Wattrus (2005) and Mooers et al. (2005) identified the mechanism of slope failure at Deer Creek. Their understanding of the stratigraphic and hydrologic stress and strength interrelationships at Deer Creek has provided the capacity for predicting slope failure in the Minnesota portion of the Nemadji River Basin.

The glacial geology of the Nemadji River basin consists of a thick sequence of lacustrine clays and clay tills interbedded with thin nearshore lacustrine sand. These nearshore sands communicate hydraulically with coarse sand and gravel sequences in the topographically higher Thomson and Nickerson Moraines (Figure 11). Potentiometric head in the confined lacustrine sands therefore reflect the elevation potential of groundwater in the moraine. The groundwater in the sand horizons is recharged in a nearby moraine 200-250 feet higher in elevation. The seepage is driven by the high hydraulic potential in local aquifers.

Results of the failure analysis agree with Mooers and Wattrus' (2005) analysis of the Deer Creek area. The problem of slope failure by slumping is the result of areas of higher slope where the artesian head exceeds the land surface. The analysis suggests that the shear strength of the clay and the driving shear stress lie very close to one another in the incised river channels of the Nemadji River basin. In areas where incision increases the slope of the land surface in excess of about 10%, the driving shear stress is greater that the shear strength of the clay and slumping is more likely to occur. Additionally, a small reduction in shear strength, from an increase in pore water pressure or a decrease in load for example, can lead to failure of the clay by slumping. Since both the Deer and Mud Creek volcano areas occur near the outer perimeter of the clay portion of the basin, this suggests that the presence of shallow confined artesian coarse-grained aquifer(s) contribute groundwater for the formation of the volcanoes.

When the potentiometric surface exceeds the land surface, the shear strength of the clay is reduced to the point where a small increase in driving stress, such as rapid draining of a beaver pond or seismic waves from dynamite (Terzaghi, 1996 p.197), may liquefy soil in banks (Terzaghi, 1996 p.267), and trigger a failure event. Fractures are may open allowing groundwater flow and loss of aquifer material.

The sediment volcanoes at Deer and Mud Creeks are likely associated with nearby slumps (Gill and Keunen, 1957). However, the exact mechanisms and pathways of groundwater and sediment discharge from the volcanoes are unknown. One possible mechanism may be groundwater under pressure is exploiting buried faults (Mooers and Wattrus, 2005) remobilized by unloading.

Another possible mechanism includes a “hanging” water table scenario. Slopes submerged during floods or high water levels are comparatively stable because the water pressure acting on the surface of the slope helps to support it (Easterbrook, 1999), i.e., the water and slope are in static equilibrium. If, however, the water level falls rapidly (as happened to the pond after removing a beaver dam at Deer Creek, or during a flooding from a rapid winter melt), the stabilizing influence of the water against the bank disappears. If the slopes consist of cohesive soils of low transmissivity, the water table may not be lowered at the same rate as the body of water, and the slope will be temporarily overloaded with excess pore water - creating a “hanging” water table (Figure 24). Examining the profiles in Figure 14, the hydraulic head near the volcano areas could conceivably drop by 1 meter over a 50 meter distance, resulting in relatively high hydraulic gradient of 0.02. The pore water reduces both cohesion and internal friction of the soil, and water pressures then act laterally toward the face of the slope. Water may liquefy sediment at depth, or it may increase the volume of clay, if present, encouraging swelling and further destabilizing the slope. Additionally the weight of the water increases the shear stress. These factors alone or together may lead to slope failure. Thus the rapid drawdown of the beaver pond may have reduced the effective strength of the Deer Creek banks, and may have been a critical factor in slope stability there.

The model in Figure 24 indicates that groundwater discharging from the sediment volcanoes may be derived locally from near the stream banks. It also implies that the focused discharge may slow when the water table equilibrates with the new pond water level controlled by the new beaver dam. However it is possible that groundwater may be coming from a deeper source that is exploiting deep fractures or highly conductive sediments at depth.

Since the sediment volcano areas at Deer and Mud Creeks occur at the toe of slumps, this may indicate that fracturing along the base of the slumps has loosened sediment and is the source of discharged sediment. The sediment and groundwater would therefore be derived from shallow aquifers near the volcanoes. Since slumping is a common occurrence in the Nemadji River basin, it is possible that other sediment volcanoes exist there.

From a geomorphological standpoint, it is a given that the Nemadji River basin will continue to contribute sediment to Lake Superior since it is topographically higher in elevation than the Lake Superior basin. Much of the Nemadji River watershed is 200-600 feet above the level of Lake Superior, so the transport of sediment in the basin to the harbor and lake will continue. The rate of sedimentation will depend somewhat on anthropomorphic activities, the amount and degree of human development, and factors such as land use conservation efforts (Reidel et al., 2002, 2005).

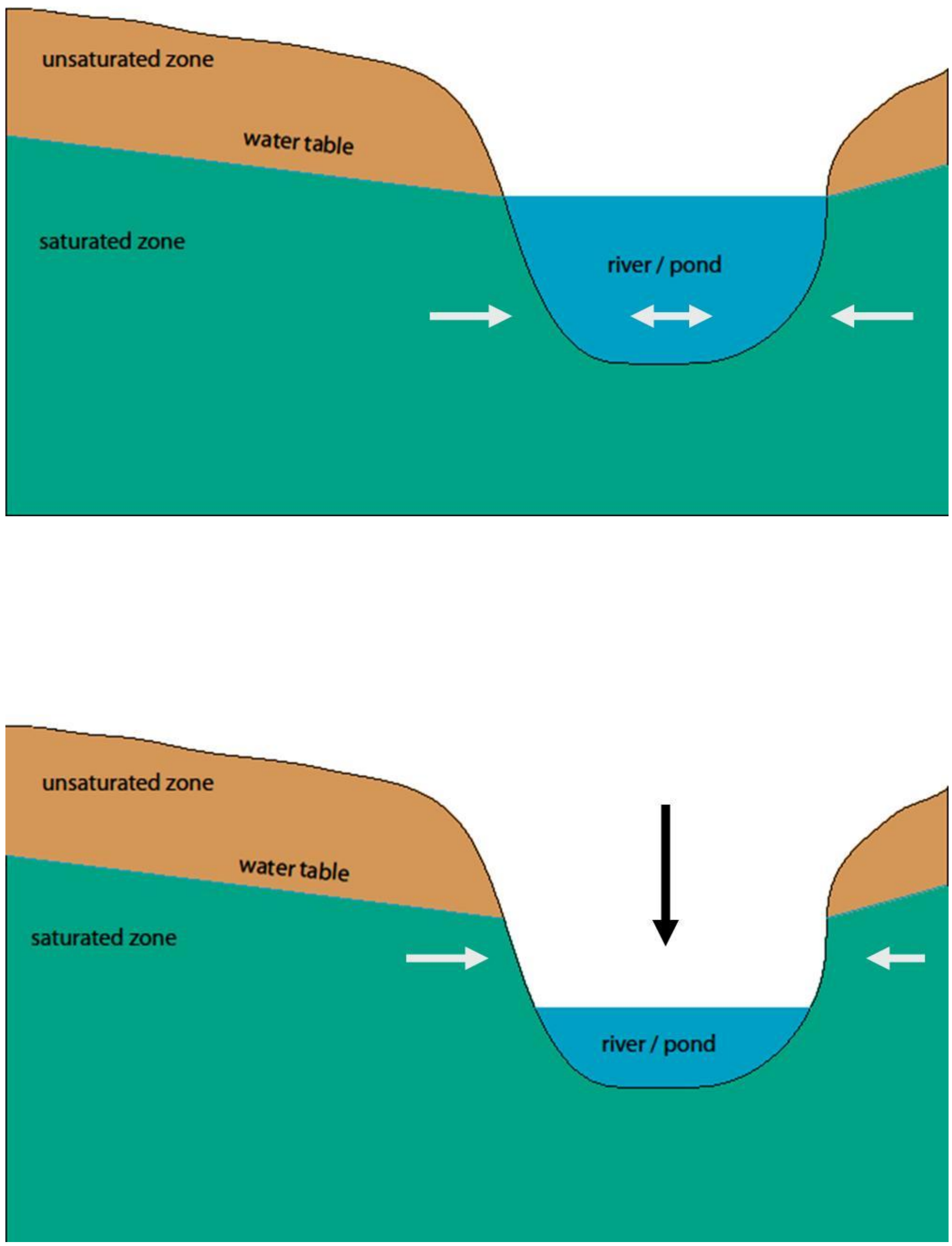

Figure 24. Rapid drawdown of a pond causing suspension of a water table.

While erosion of sediment in the Nemadji River basin is a natural process, humans have accelerated erosion rates since settlement in the last 200 years through logging, conversion of forest to agricultural land, and forest fires (NRCS 1998, Reidel 2002). These processes serve to produce flashier, more rapid runoff, which increases erosion rates. A model for erosion susceptibility would help land use managers mitigate these problems.

There are few options to mitigate the problem of sediment loading into the Nemadji's streams from erosion and sediment volcanoes. To mitigate the problem of sediment loading due to bank erosion in the Nemadji River basin, slope control (Andrews, et al, 1980), vegetation stabilization, and land use management (Banks and Brooks, 1992) appear to be the most feasible options. These solutions may also reduce the potential for sediment volcano formation.

To mitigate sediment loading from the volcanoes, solutions could include lowering the hydraulic head in the vicinity of problematic groundwater seepages using extraction wells (Kappel et al., 1996; Mooers and Wattrus, 2005); rerouting steams away from problematic areas (Kappel et al., 1996), and construction of retention dams to retain sediment and raise the hydraulic head in those areas (Kappel et al., 1996). The latter appears to be currently happening at Deer Creek with the re-establishment of a beaver dam directly downstream of the sediment volcano area which has raised the hydraulic head in the pond behind the dam by approximately 4 feet, submerging most of the sediment volcanoes there. Eventually the system at Deer Creek should reach equilibrium between driving forces causing failure and resisting forces stabilizing the clay, at which time seepage will likely slow.

The unique set of conditions that led to failure at Deer Creek have allowed development of a predictive basin-wide model of slope instability that can be used by governmental agencies for cost-effective environmental management and protection. This investigation has identified potential problem areas and will aid government officials in managing development and construction projects in the area that will prevent further problems with slope failure, erosion, and turbidity. Results of this study can be used to educate land-use managers and other stakeholders on the existing conditions and ways to mitigate future problems.

This project can impact the coastal resources of the Lake Superior basin by providing planners and developers information to prevent unnecessary amounts of sedimentation from reaching the basin's tributaries, bays, estuaries, and the lake itself. Reduced sedimentation would require less dredging, reducing taxpayer's costs and limiting re-suspension of pollutants in the Duluth-Superior harbor. Fisheries could be enhanced by improving spawning beds in both the tributaries and the lake environment. The project can help Nemadji watershed streams aesthetically by providing a tool to help protect their natural clarity.

The factors used to calculate shear stress are relatively unchanging, so there should be a high confidence level in the shear stress results. In contrast, the factors used to calculate shear strength can vary widely just by merely by changing the cohesion variable. The model developed for this project correlates well with areas of high slope, high hydraulic potential, mapped slumps, and the SINMAP model. This correlation suggests that the model does not overpredict failure succeptibility.

This model provides a good first approximation of slumping potential, and satisfies the project objective of developing a quantitative predictive model for the red clay area of the Nemadji River basin, showing susceptibility of the land surface to slumping and thus sediment volcanoes and enhanced erosion rates.

This study can assist stakeholders in making land use decisions in the areas of agriculture, forest, riparian, fisheries, and urban/infrastructure management by providing a quantitative model of susceptibility to erosion of sediment in the Nemadji River basin. The results can be used in conjunction with other studies to help understand and reduce erosion in the basin.

Recommendations for Future Work

Testing of the predictive model developed in this study could be accomplished through further field reconnaissance of locations of groundwater springs and seeps, especially near the visibly turbid Rock Creek, which is located between Deer and Mud Creeks. Rock Creek is also one of the tributaries investigated by Wold (1994). Wold (1994) identified 39 slumps in the Rock Creek watershed.

Testing could also be accomplished through further analysis of aerial photography, and comparison to other models for the appropriate scales, such as landslide density analysis, qualitative landslide hazard analysis, or bivariate statistical landslide hazard analysis.

Further refinement of the model could be accomplished through integration and or comparison to other data, including landuse basemaps, groundwater models. Future work could include analysis of seasonal discharge from the sediment volcanoes, and isotope analysis of tritium in groundwater to help determine the origin of and residence time of the groundwater discharging from the sediment volcanoes. Soil borings and geophysical investigations could be used to characterize the local geology, especially at the sediment volcano areas. A higher-resolution digital elevation model would help improve the precision of the results. The model can be uploaded to a public GIS such as Google™ Earth.

REFERENCES

Albrecht, D.R., Brown, E.T., Swenson, J.B., Wattrus, N.J., & Parker, G., 2002. The Fate of Nemadji River Sediment in Western Lake Superior.

Allen, C.C., Oehler, D.Z., and Baker, D.M., 2009. Mud Volcanoes - A New Class Of Sites For Geological And Astrobiological Exploration Of Mars, 40th Lunar and Planetary Science Conference, poster presentation.

Andrews, S.C., Christensen, R.G., Wilson, C.D., 1980. Impact of Nonpoint Pollution Control on Western Lake Superior. Red Clay Project Final Report Part III. US Environmental Protection Agency Report, EPA. 905/9-76-002.

Bacig, E.J., 1993. Nemadji River Watershed—Carlton County 1:50,000 Map of Surficial Glacial Geology.

Baird, W.F. & Associates Coastal Engineers Ltd., August, 2000. Nemadji River Basin Sediment Transport Modeling For Two Subwatersheds.

Banks, G., Brooks, K.N., 1992. Erosion—Sedimentation and Nonpoint Pollution in The Nemadji Watershed: Status of Our Knowledge. Completion Report to the Carlton County Soil and Water Conservation District, Carlton, Minnesota.

Bluemle, J. P., 1993. Hydrodynamic blowouts in North Dakota: in Aber, J. S. (ed), Glaciotectonic and Mapping Glacial Deposits: Proceedings of the INQUA Commission on Formation and Properties of Glacial Deposits: Canadian Plains Research Center, Univ. of Regina, 259 - 266 p.

Boerboom, T.J., Project Manager, 2002. Contributions to the Geology of Pine County, Minnesota: Minnesota Geological Survey Report of Investigations 60, 91.p.

Boerboom, T.J., 2009. Bedrock Geology, pl. 2, of Boerboom, T.J., project manager, Geologic Atlas of Carlton County, Minnesota: Minnesota Geological Survey County Atlas C-19, pt. A, 6 pls., scale 1:100,000.

Bolt, B.A., 1993. Earthquakes and Geological Discovery, Scientific American Library, p. 172.

Bridges, T.S., et al., 2008. The Four Rs of Environmental Dredging: Resuspension, Release, Residual, and Risk. U.S. Army Corps of Engineers Dredging Operations and Environmental Research Program, ERDC/EL TR-08-4.

Carlton County Water Plan Advisory Committee, 2000. Nemadji River Basin Project Phase II Workplan.

Carlton County Soil Water Conservation District, 2005. Nemadji River Basin Project Newsletter Summer 2005.

Carney, S.C., 1996. Paleohydrology of the Western Outlets of Glacial Lake Duluth; [M.S. Thesis] University of Minnesota, Duluth, 129 p.

Clayton, L., and Moran, S. R., 1982. Chronology of late Wisconsinan Glaciation in Middle North America: Quaternary Science Reviews, v. 1, p. 55–82.

Clayton, L., 1984. Pleistocene Geology of the Superior Region, Wisconsin: Wisconsin Geological and Natural History Survey, Information Circular 46, 40 p.

Corthay, J.E., II, and Aliyev, A. A., 2000. Delineation of a Mud Volcano Complex, Surficial Mudflows, Slump Blocks, and Shallow Gas Reservoirs, Offshore Azerbaijan. Offshore Technology Conference, 1 May- 4 May, 2000, Houston, TX.

Cutler, P.M., Mickelson, D.M., Colgan, P.M., Mac-Ayeal, D.R., and Parizek, B.R., 2001. Influence of the Great Lakes on the dynamics of the southern Laurentide ice sheet: Numerical experiments, Geology vol. 29 p.1039-1042.

Davidson D. W., Kapustka L.A., and Koch R.G. 1977. The Influence of Vegetation on Red Clay Erosion in the Nemadji River Basin. Bulletin Ecological Society of America. Vol. 58 No. 2.

Duluth News-Tribune, 2009. Dredging concerns halt harbor digging. By Sam Cook, June 17, ed. 2 p.

Duluth-Superior Metropolitan Interstate Council, 2007. Erie Pier Management Plan.

Easterbrook, D.J., 1999. Surface Processes and Landforms, 2nd Ed. Prentice Hall, Upper Saddle River, New Jersey, 546 p.

Farrand, W.R., 1960. Former shorelines in western and northern Lake Superior basin, Ph.D. dissertation, Univ. Michigan, Ann Arbor, MI.

Farrand, W.R., 1969. The Quaternary history of Lake Superior. In Proceedings of the 12th Conference on Great Lakes Research, International Association of Great Lakes Research, pp. 181–197.

Farrand, W.R. and Drexler, C.W., 1985. Late Wisconsinan and Holocene History of the Lake Superior Basin, in Karrow, P.F. and Calkin, P.E., eds., Quaternary Evolution of the Great Lakes: Geological Association of Canada, Special Paper 30, p. 17-32.

Gill, W. D., Kuenen, P. H., 1957. Sand volcanoes on slumps in the Carboniferous of County Clare, Ireland. Quarterly Journal of the Geological Society 113: 441-460.

Guhman, A. I., and Pederson, D. T., 1992. Boiling sand springs, Dismal River, Nebraska: Agents for formation of vertical cylindrical structures and geomorphic change Geology; 20: p. 8 - 10.

Hobbs, H.C., and Goebel, J.E., 1982. Geologic Map of Minnesota, Quaternary Geology Map S-1, University of Minnesota, Minnesota Geological Survey.

Iverson, R.M., 2000. Landslide triggering by rain infiltration, Water Resources Research v. 36, n.7, p. 1897-1910.

Johnson, M.D., 1986. Pleistocene Geology of Baron County, Wisconsin: Wisconsin Geologic and Natural History Survey, Information Circular 55. 42 p.

Johnson, M.D. & Mooers, H.D., 1998. Ice-margin positions of the Superior Lobe during Late Wisconsinan deglaciation. In: Patterson, C.J. & Wright, H.E., Jr. (eds), Contributions to Quaternary studies in Minnesota. Minnesota Geological Survey Report of Investigations, 49, 7-14.

Kappel, W.M., Sherwood, D.A., and Johnston, W.H., 1996. Hydrogeology of the Tully Valley mudboils and characterization of mudboil activity, Onondaga County, New York: U.S. Geological Survey Water-Resources Investigations Report 96-4043, 71 p.

Knaeble, A.R, and Hobbs, H.C., 2009. Surficial Geology, pl. 3, of Boerboom, T.J., project manager, Geologic Atlas of Carlton County, Minnesota: Minnesota Geological Survey County Atlas C-19, pt. A, 6 pls., scale 1:100,000.

Krahn J., 2003. The 2001 R.M. Hardy Lecture: The limits of limit equilibrium analyses. Canadian Geotechnical Journal, Volume 40, Number 3, 1, pp. 643-660.

Lannon, P.M., 1986. The Quaternary Stratigraphy and Glacial history of the Duluth-Superior area: [M.S. Thesis] University of Minnesota, Duluth, 115 p.

Leverett, F., 1929. Moraines and shore lines of the Lake Superior region, U.S. Geological Survey Professional Paper 154-A, p. 1-72.

Li, Y., Craven, J., Schweig, E., and Obermeier, S., 1996. Sand boils induced by the 1993 Mississippi River flood: Could they one day be misinterpreted as earthquake-induced liquefaction? Geology; v. 24, p. 171-174,

Magner, J. A., & Brooks, K. N., 2008. Predicting stream channel erosion in the lacustrine core of the upper Nemadji River, Minnesota (USA) using stream geomorphology metrics. *Environmental Geology*, *54*, p. 1423–1434.

Meyer, G.N., 1986. Subsurface till stratigraphy of the Todd County area, central Minnesota, Minnesota Geological Survey Report of Investigations no. 34, 40 p.

Meyer, G.N., and Knaeble, A.R., 1996. Quaternary geology of Stearns County, Minnesota, In Meyer, G.N., and Swanson, L., editors, Text supplement to the Geologic Atlas, Stearns County, Minnesota Geological Survey County Atlas Series C-10, p. 16-39.

Mickelson, D.M., Clayton, L., Fullerton, D. S., and Borns, H. W. Jr., 1983. The Late Wisconsin glacial record of the Laurentide Ice Sheet in the United States, in Porter, S.C., ed. The Late Pleistocene: Minneapolis, University of Minnesota Press, p. 3-37.

Milkov, A.V., 2000. Worldwide distribution of submarine mud volcanoes and associated gas hydrates, Marine Geology, Volume 167, Issues 1-2, 15 June, p. 29-42.

Minnesota Department of Natural Resources, 1996. Geomorphology of Minnesota, Data Deli, http://deli.dnr.state.mn.us.

Minnesota Geological Survey and Minnesota Department of Health County Well Index, http://www.geo.umn.edu/mgs/cwi.html, http://www.health.state.mn.us/divs/eh/cwi/index.html.

Minnesota Pollution Control Agency and Wisconsin Department of Natural Resources, 1992. St. Louis River System Remedial Action Plan, Stage One.

Minnesota Pollution Control Agency, 2004. Draft List of Impaired Waters, http://www.pca.state.mn.us/water/tmdl/tmdl-303dlist.html.

Minnesota Pollution Control Agency, 2008. Background on Total Maximum Daily Loads, General Public: gp5-13.

Montgomery, D.R. and Dietrich, W.E., 1994. A physically based model for topographic control on shallow landsliding, Water Resources Research, v. 30, n. 4, p. 1153-1171.

Mooers, H.D., 1988. Quaternary history and ice dynamics of the late Wisconsin Rainy and Superior lobes, central Minnesota [Ph.D. Thesis]: Minneapolis, University of Minnesota, 200 p.

Mooers, H.D., 1996a. Geomorphology of the Duluth 1:100,000 quadrangle and the development of the Land Type Association layer of the Ecological Classification System, Minnesota Department of Natural Resources - Division of Forestry.

Mooers, H.D., 1996b. Geomorphology of the Sandstone 1:100,000 quadrangle and the development of the Land Type Association layer of the Ecological Classification System, Minnesota Department of Natural Resources - Division of Forestry.

Mooers, H.D., and Lehr, J.D., 1997. Terrestrial record of Laurentide Ice Sheet reorganization during Heinrich events, Geology, vol. 25, p. 987-990.

Mooers, H.D., and Wattrus, N.L., 2005. Results of Deer Creek Groundwater Seepage Investigation Report to Carlton County Planning and Zoning Department, 29p.

Mooers, H.D., Wattrus, N.L., and Mossberger, I.G., 2005. Regional groundwater control of slope stability in the Glacial Lake Duluth Basin, Minnesota, Geological Society of America Abstracts with Program, vol. 37, no. 7, p. 391.

Morrissey, M.M., Wieczorek, G.F., and Morgan, B.A., 2001. A Comparative Analysis of Hazard Models for Predicting Debris Flows in Madison County, Virginia, U.S. Geological Survey Open-File Report 01-0067.

Morey, G.B., 1967. Stratigraphy and Petrology of the Type Fond du Lac Formation, Duluth, Minnesota: Minnesota Geological Survey Report of Investigations 7, 35 p.

Morey, G.B., and Ojakangas, R.W., 1970. Sedimentology of the Middle Precambrian Thomson Formation, east-central Minnesota: Minnesota Geological Survey Report of Investigations 13, 32 p.

Natural Resources Conservation Service, 1996. Memorandum.

Natural Resources Conservation Service and U.S. Forest Service, 1998. Executive summary report: Erosion and sedimentation in the Nemadji River Basin: Nemadji River Basin Project, 16 p.

Nemadji River Basin Project (NRBP), 2004. Newsletter Summer 2004 Issue 8.

Nemadji River Basin Project (NRBP), 2005. Newsletter Summer 2005 Issue 10.

Ojakangas, R.W., and Matsch, C.L., 1982. Minnesota's geology: Minneapolis, Minnesota, University of Minnesota Press.

Olcott, P.G., Ericson, D.W., Felsheim, P.E., Broussard, W.L., 1978. Water resources of the Lake Superior watershed, Northeastern Minnesota. Hydrologic Investigations Atlas, US Geological Survey, Department of the Interior and the Minnesota Department of Natural Resources, Division of Water, Soil, and Minerals, HA-582.

Olsen, B.M., and Mossler, J.H., 1982. Depth to Bedrock, Geologic Map of Minnesota, Minnesota Geological Survey, Map S-14.

Pack, R.T., Tarboton, D.G., Goodwin, C.N., 1999. GIS-based landslide susceptibility mapping with SINMAP, Proceedings of the 34th Symposium on Engineering Geology and Geotechnical Engineering, Bay, J.A. (editor), 34, p.219-231.

Patterson, C.J., and Knaeble, A.R., 2001. Surficial geology, pl. 4 of Boerboom, T.J., project manager, Geologic Atlas of Pine County, Minnesota: Minnesota Geological Survey County Atlas C-13, pt. A, 7 pls., scale 1:100,000.

Raymahashay, B., 1968. A geochemical study of rock alteration by hot springs in the Paint Pot Hill area, Yellowstone Park, Geochimica et Cosmochimica Acta, Volume 32, Issue 5, May 1968, Pages 499-522.

Riedel, M. S., 2000. Geomorphic impacts of land use on clay channel streams [Ph.D. thesis], University of Minnesota, 283 pages.

Riedel, M. S., Verry, E. S., and Brooks, K., 2002. Land use impacts on fluvial processes in the Nemadji River watershed. Hydrological Science and Technology, 18 (1-4):197-205.

Riedel, M.S., Verry, E.S., Brooks, K.N., 2005. Impacts of land use conversion on bankfull discharge and mass wasting. Journal of Environmental Management, Vol. 76, no. 4, pp. 326-337. Sep 2005.

Robinson, L., ed., 2005. Field trip guidebook for selected geology in Minnesota and Wisconsin. Prepared for the 2005 Geological Society of America North Central Section Meeting, Minneapolis, Minnesota, May 18-20, 2005. 278 p.

Saucier, R. T., 1989. Evidence for episodic sand-blow activity during the 1811-1812 New Madrid (Missouri) earthquake series. Geology; 17: 103 - 106.

Strachan, L.J., 2002. Slump-initiated and controlled syndepositional sandstone remobilization: an example from the Namurian of County Clare, Ireland. Sedimentology,49:1, pp 25-41.

Streitz, A., and Hansen, D., 2006, Volcanoes return to Northeastern Minnesota, Minnesota Ground Water Association Newsletter, Vol. 25, No. 3.

Swenson, K., 2008. Deer Creek/Nemadji River Total Maximum Daily Load Summary of Existing Water Quality Data, Carlton County Soil and Water Conservation District.

Sydor, et al., 1979. Red Clay Turbidity and its Transport in Lake Superior, Great Lakes National Program Office, EPA-905/9-79-004.

Terzaghi, K., Peck, R.B., and Gholamreza, M., 1996, Soil Mechanics In Engineering Practice, New York, Wiley, 549 p.

Todd County GIS Department, 2002. Erosion Susceptibility and Water Orientation, Sauk River Watershed District. Map, 1 p.

Upham, W., 1920. Minnesota Place Names, 3rd ed., St. Paul: Minnesota Historical Society Press, 2001.

US Army Corps of Engineers (USACE), 2003. Engineering and Design Slope Stability Manual, EM 1110-2-1902.

Weppner, E., Hoyt, J., and Haneberg, W. C., 2008. LiDAR-based landslide hazard modeling using PISA-m, SHALSTAB, and SMORPH, Freshwater Creek and

Ryan Slough watershed, Humboldt County, California, American Geophysical Union, Fall Meeting 2008, abstract #H41K-04.

Winchell, N.H., 1901. Glacial lakes of Minnesota, Geological Society of America Bulletin, Vol. 12, p. 109-128.

Wirth, K.R., Vervoort, J.D., and Naiman, Z.J. 1997. The Chengwatana Volcanics, Wisconsin and Minnesota: petrogenesis of the southernmost volcanic rocks exposed in the Midcontinent rift. Canadian Journal of Earth Sciences, 34: 536–548.

Wold, W.L., 1994. Soil mass movement in the Nemadji River watershed, [M.S. Thesis], University of Minnesota, 1994.

Wright, H.E., Jr., 1964. The classification of the Wisconsin Glacial Stage: Journal of Geology v. 72, no. 5. p. 628-637.

Wright, H.E., Jr., Watts, WA, 1969. Glacial and Vegetational History of Northeastern Minnesota, University of Minnesota.

Wright, H.E., Jr., Mattson, L.A., Thomas, J.A., 1970. Geology of the Cloquet Quadrangle, Carlton County, Minnesota: Minnesota Geological Survey Geologic Map GM-3 (with text), 30p.

Wright, H.E., Jr., 1972. Quaternary History of Minnesota, in Sims, P. K. and Morey, G. B., eds., Geology of Minnesota: A Centennial Volume: Minneapolis, Minnesota Geological Survey, p. 515-547.

Wright, H.E. Jr., Matsch, C.L., and Cushing, E.J., 1973a. The Superior and Des Moines Lobes, In Black, R.F., Goldthwait, R.P., and Willman, G.B., eds., The Wisconsinan Stage: Geological Society of America Memoir 136, p. 153-185.

Wright, H.E. Jr., 1973b. Tunnel Valleys, Glacial Surges, and Subglacial Hydrology of the Superior Lobe, Minnesota. In Black, R.F., Goldthwait, R.P., and Willman, G.B., eds., The Wisconsinan Stage: Geological Society of America Memoir 136, p. 251-276.

Zarth, R.J., 1977. The Quaternary geology of the Wrenshall and Frogner quadrangles, northeastern Minnesota. [M.S. thesis], University of Minnesota, 93 p.

APPENDIX A Review of Applicable Mass Wasting Analysis Methods

There are many types of mass wasting and many methods of analysis so a complete review is not presented here. The methods applicable to this project include slope stability, landslide potential, and soil erodibility models as well as field and laboratory measurements.

Most slope stability analyses for engineering design considerations are performed in two-dimensional vertical cross-section (USACE, 2003). A factor of safety (FoS) is calculated by dividing the forces resisting movement (friction, cohesion) by the forces driving movement (gravity); i.e., the ratio of shear strength to shear stress. If the FoS exceeds a value of one, the slope is stable; if less than one – unstable; if close to or equal to one, metastable.

Slope stability methods are based on the Mohr-Coulomb equation. Slope stability methods are deterministic and are called limit equilibrium methods when a state is achieved where the system is at the verge of failure. The methods involve dividing the sliding mass above the failure surface into a number of slices. Then a circular or wedge-shaped failure surface is designated, and the stress along each vertical slice is summed. The forces acting on each slice are obtained by calculating the mechanical equilibrium for the slices. Some of the methods merely estimate stress based on a desired FoS (i.e., back-calculated). Some popular methods include the Fellenius Method, Bishop, Spencer, Modified Swedish, and Wedge methods (USACE, 2003). By making some simplifying assumptions, the problems become statically determinate and suitable for hand calculations. The fundamental shortcoming of limit equilibrium methods, which only satisfy equations of statics, is that they do not consider strain and displacement compatibility. This limitation can be overcome by using finite element analysis (Krahn, 2003). Probablilistic methods and reference charts are also used for slope stability analysis.

Currently there are numerous software models used to predict landslide potential. The models commonly use a form of the Mohr-Coulomb method with an infinite slope, and disregard cohesion. One model is the Stability Index Mapping (SINMAP) model. SINMAP is used for identification of potentially unstable zones in large land areas (Pack et al., 1998). The model estimates shallow translational landslides by combining the infinite slope-stability equation with a steady-state hydrology model that calculates depth of saturation based on water recharge rate and soil transmissivity of water. Other models include SHALSTAB (shallow slope stability) (Montgomery & Dietrich, 1994), PISA-m, and SMORPH (Weppner et al, 2008). The SINMAP, and SHALSTAB models assume steady state, saturated flow parallel to the slide surface and use Darcy's law for estimating the spatial distribution of pore pressures. A model by Iverson (2000) considers transient unsaturated flow and uses the Richards equation for estimating soil pore pressure response at depth (Morrisey, 2001).

Physical models allow for relatively fine-scale hazard mapping (Pack et al., 1998) and tend to be less site-specific than multivariate statistical analyses (Montgomery and Dietrich, 1994). Model parameters commonly include cohesion due to roots and soil, slope of the land surface, saturated bulk density of the soil, soil thickness above the failure plane, saturated soil thickness above the failure plane, and soil angle of friction in degrees.

To illustrate the variability and difficulty that can occur in slope stability modeling, in one study (Weppner et al, 2008) three different models were applied to a TMDL study area in a forested area of California. Two of the models identified 75% of field or remote sensing-inventoried landslides while the third identified 99% of the landslides, but at a cost of predicting three times more unstable ground than the other two models.

Analysis of landslide hazards using GIS techniques normally take into account factors such as size of the study area, rainfall, slope, elevation, aspect, soil type, vegetation, geomorphological units, etc. Different landslide GIS analysis techniques are applicable to study areas of differing scales. Since the Nemadji River basin covers approximately 433 square miles, the watershed would be considered a medium-to-large area study scale for GIS landslide evaluation purposes. Some methods include landslide distribution, activity, density, and frequency analysis; geomorphic and qualitative landslide hazard analysis; bivariate, multivariate, and deterministic hazard analysis; and the likelihood ratio approach.

Semi-quantitative methods can combine areal factors such as land use (i.e., urban, agricultural, etc.) with other factors such as slope to broadly rate erosion succeptiblity as high or low (e.g., Todd County, 2002).

Soil erodibility models such as the Universal Soil Loss Equation (USLE) generally calculate erosion rates or volumes, not locations. The erodibility of soils can be described as their sensitivity to the effects of water on the soil structure. This property is expressed as an erodibility index, determined by combining the effects of slope and soil type, rainfall intensity and land use.

Shear strength, rather than being calculated, can also be measured in the laboratory using triaxial compression or direct shear test equipment, and directly in the field using vane shear testing equipment (Terzaghi, 1996).

Other non-modeling mass wasting analyses include field identification, remote sensing identification, and empirical field methods such as erosion pin measurements.

APPENDIX B RockWorks Model Menu Summary

Menu Title = "Lithology Modeling Options ..."

Lithology Modeling Options

Create New Model .... (LITHOMOD,CREATE_NEW_MODEL)

Spatial (XYZ) Filtering .... False (SPATIAL_FILTER,ACTIVE)

X (Easting) Filter .... False (SPATIAL_FILTER,X_FILTER)

Minimum X .... 0.0 (SPATIAL_FILTER,X_MIN)

Maximum X .... 100.0 (SPATIAL_FILTER,X_MAX)

Y (Northing) Filter .... False (SPATIAL_FILTER,Y_FILTER)

Minimum Y .... 0.0 (SPATIAL_FILTER,Y_MIN)

Maximum Y .... 100.0 (SPATIAL_FILTER,Y_MAX)

Z (Elevation) Filter .... False (SPATIAL_FILTER,Z_FILTER)

Minimum Z .... 0.0 (SPATIAL_FILTER,Z_MIN)

Maximum Z .... 100.0 (SPATIAL_FILTER,Z_MAX)

Upper Surface Filter .... True (SPATIAL_FILTER,UPPER_SURFACE_FILTER)

Grid File .... C:\ RockWorks\Surface.grd (SPATIAL_FILTER,UPPER_SURFACE_GRID)

Lower Surface Filter .... False (SPATIAL_FILTER,LOWER_SURFACE_FILTER)

Grid File .... C:\ RockWorks2006\Samples*.grd (SPATIAL_FILTER,LOWER_SURFACE_GRID)

Remove Duplicates .... True (SPATIAL_FILTER,REMOVE_DUPLICATES)

Create Filtering / Sampling Report True (LITH_REPORT,SHOW_REPORT)

Lithology Model Name .... C:\ \RockWorks\Lith02.mod (LITHOMOD,NEW_MODEL_NAME)

Model Dimensions

"Hardwire" Project Dimensions .... True (PROJECT,HARDWIRE_DIMENSIONS)

Adjust Project Dimensions ....
(PROJECT_DIMENSIONS,PROJECT_DIMENSIONS)
Variable (Data Specific) Dimensions (PROJECT,HARDWIRE_DIMENSIONS)
Grid Dimensions
Average Minimum Distance .... 1 (GRIDSIZE,DIMENSIONING_METHOD)
Scalar .... 1.0 (GRIDSIZE,AVE_MIN_DISTANCE_SCALER)
Manual .... (GRIDSIZE,DIMENSIONING_METHOD)
Node Density .... 50 (GRIDSIZE,NODE_DENSITY)
Current .... (GRIDSIZE,DIMENSIONING_METHOD)
Solid Dimensions
Horizontal (X/Y) .... 50 (SOLID_RESOLUTION,HORIZONTAL_DENSITY)
Vertical (Z) .... 50 (SOLID_RESOLUTION,VERTICAL_DENSITY)
Confirm Model Dimensions .... False (PROJECT,CONFIRM_DIMENSIONS)
Randomize Blending .... True (LITHOMOD,RANDOMIZE)
Interpolate Outliers .... True (LITHOMOD,INTERPOLATE_OUTLIERS)
Tilted Modeling .... False (MODEL_TILTING,TILT)
Dip Direction .... 0.0 (MODEL_TILTING,DIP_DIRECTION)
Dip Amount (Negative) .... 0.0 (MODEL_TILTING,DIP_AMOUNT)
Warp Model Based On Grid .... False (MODEL_WARPING,WARP)
Grid Model .... C:\ \RockWorks\Surface.grd
(MODEL_WARPING,GRID_NAME)
Upper Surface (Grid) Filter .... True (STRATABOUND,UPPER_FILTER)
Grid Model .... C:\ RockWorks\Surface.grd
(STRATABOUND,SUPERFACE_GRID)
Buffer Size .... 1.0 (STRATABOUND,SUPERFACE_BUFFER_SIZE)
Lower Surface (Grid) Filter .... False (STRATABOUND,LOWER_FILTER)
Grid Model .... C:\ RockWorks2006\Samples\Subface01.grd
(STRATABOUND,SUBFACE_GRID)
Buffer Size .... 1.0 (STRATABOUND,SUBFACE_BUFFER_SIZE)

Undefined Node Value (Value to assign to undefined/filtered nodes.)
Null (-1.0e27) .... True (NULL,SET_UNDEFINED_TO_NULL)
User-Defined .... (NULL,SET_UNDEFINED_TO_NULL)
Replacement Value .... 0.0 (NULL,UNDEFINED_G_VALUE)
Use Existing Model .... False (LITHOMOD,CREATE_NEW_MODEL)
Model Name .... C:\ RockWorks\Lith02.mod
(LITHOMOD,OLD_MODEL_NAME)
Create Diagram .... True (LITHOMOD,CREATE_DIAGRAM)
Voxel Style
Full Voxel .... 1 (LITHOMOD,VOXEL_STYLE)
Midpoint .... (LITHOMOD,VOXEL_STYLE)
Plot Logs .... False (ADD_3D_LOGS,PLOT_LOGS)
Adjust Striplog Settings .... (3D_LOG_OPTIONS,3D_LOG_OPTIONS)
Reference Cage .... True (CAGE,PLOT_CAGE)
Plot Panels .... False (CAGE,PLOT_PANELS)
Color .... 65,535 (CAGE,PANEL_COLOR)
Plot Lines .... True (CAGE,PLOT_LINES)
Line Style .... Solid/1/DKGRAY (CAGE,LINE_LTYPE)
Plot Labels .... True (CAGE,PLOT_LABELS)
Font .... Arial/10/Black/-90 (CAGE,FONT)
Offset .... 3.0 (CAGE,LABEL_OFFSET)
Plot Leader Lines .... True (CAGE,PLOT_LEADERS)
Horizontal (XY) Decimal Places
Automatic .... True (CAGE,AUTOMATIC_HORIZONTAL_DECIMALS)
Manual .... (CAGE,AUTOMATIC_HORIZONTAL_DECIMALS)
Decimal Places .... 1 (CAGE,HORIZONTAL_DECIMALS)
Vertical (Z) Decimal Places
Automatic .... True (CAGE,AUTOMATIC_VERTICAL_DECIMALS)
Manual .... (CAGE,AUTOMATIC_VERTICAL_DECIMALS)

Decimal Places .... 1 (CAGE,VERTICAL_DECIMALS)

North .... True (CAGE,NORTH)

South .... True (CAGE,SOUTH)

West .... True (CAGE,WEST)

East .... True (CAGE,EAST)

Base .... True (CAGE,BASE)

Top .... True (CAGE,TOP)

Dimensions

Project Dimensions .... 0 (CAGE,DIMENSION_METHOD)

Adjust Project Dimensions ....

(PROJECT_DIMENSIONS,PROJECT_DIMENSIONS)

Automatic .... (CAGE,DIMENSION_METHOD)

Manual .... (CAGE,DIMENSION_METHOD)

X (Easting)

Minimum (West) .... 652,660.0 (CAGE,X_MIN)

Maximum (East) .... 653,600.0 (CAGE,X_MAX)

Spacing .... 100.0 (CAGE,X_SPACING)

Y (Northing)

Minimum (South) .... 5,535,000.0 (CAGE,Y_MIN)

Maximum (North) .... 5,535,980.0 (CAGE,Y_MAX)

Spacing .... 100.0 (CAGE,Y_SPACING)

Z (Elevation)

Minimum (Base) .... 1,230.0 (CAGE,Z_MIN)

Maximum (Top) .... 1,500.0 (CAGE,Z_MAX)

Spacing .... 50.0 (CAGE,Z_SPACING)

Include Lithology Legend .... True (3D_LITH_LEGEND,INCLUDE)

Size .... 0.8 (LEGEND_3D,SCALER)

Font .... Arial/9/0 (LEGEND_3D,FONT)

Position

Left .... 1 (3D_LITH_LEGEND,POSITION)

Right .... (3D_LITH_LEGEND,POSITION)

Offset

Horizontal .... 0.0 (3D_LITH_LEGEND,X_OFFSET)

Vertical .... 0.0 (3D_LITH_LEGEND,Y_OFFSET)